



# Seasonal dynamics of dissolved organic matter along an intertidal gradient in semi-arid mangrove soils (New Caledonia)

Naïna Mouras<sup>1,2</sup>, Cyril Marchand<sup>1</sup>, Maximilien Mathian<sup>1</sup>, Hugues Lemonnier<sup>2,3</sup>

<sup>1</sup>Institute of Applied and Exact Sciences, University of New Caledonia, Noumea, New Caledonia

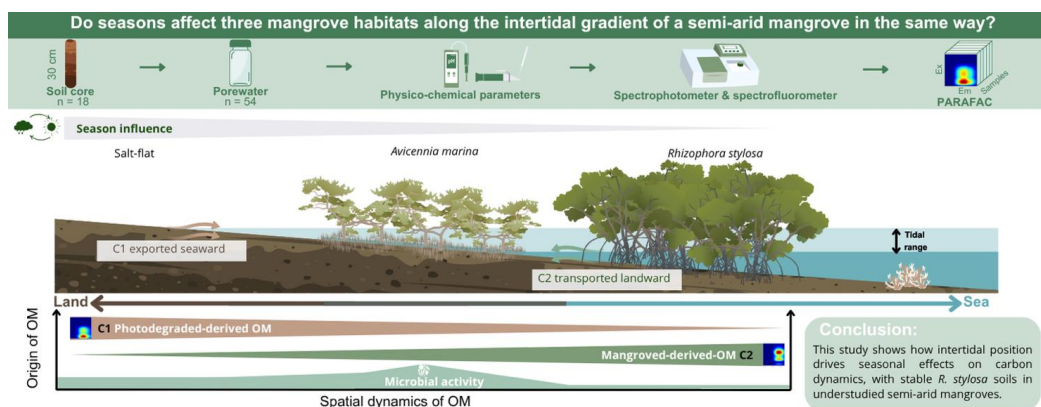
<sup>2</sup>Ifremer, CNRS, IRD, Univ Nouvelle-Calédonie, Univ La Réunion, ENTROPIE, 98800 Nouméa, New Caledonia

<sup>3</sup>MARBEC, Univ. Montpellier, CNRS, Ifremer, IRD, Sète, France

Correspondence to: Naïna Mouras ([naina.mouras@ifremer.fr](mailto:naina.mouras@ifremer.fr) ; [naina.mouras@unc.nc](mailto:naina.mouras@unc.nc))

**Abstract.** Mangrove ecosystems play a key role in the global carbon cycle notably through the production, transformation, and export of dissolved organic matter (DOM). If DOM export to adjacent ecosystems is well studied, its dynamics in mangrove soils remain poorly understood. In this study, DOM quantity and quality were investigated in semi-arid mangroves with no external organic matter input, developing along an intertidal gradient: a salt-flat, an *Avicennia marina* stand, and a *Rhizophora stylosa* stand. Soil and porewater samples were collected during both wet and dry seasons, and analysed for physicochemical parameters, total and dissolved organic carbon (TOC, DOC), chromophoric and fluorescent dissolved organic matter (CDOM, FDOM), and mineralogical composition. Our result show distinct DOM quantity and quality between habitats. The *Rhizophora stylosa* stand, characterized by daily tidal immersion and the lowest salinity, presented high and stable DOC concentrations throughout the year. The dominance of one humic-like fluorescent component suggests that soil DOM is primarily mangrove-derived. In this stand, tidal fluctuations are a major cause for continuous Fe reduction-oxidation cycles, which can influence DOM dynamics. In the salt-flat and the *Avicennia marina* stand, which suffer from water stress due to their position, significant seasonal variations were measured with higher DOC concentrations during the wet and warm season as a result of enhanced microbial activity. In these stands due to a more open canopy cover, DOM also originates from biological activity, as evidenced by enhanced microbially-derived fluorescent component. In addition, photodegradation can occur. These findings provide new insights into DOM cycling in mangrove soils and highlight the combined effects of zonation and seasons.

**Keywords:** Porewater, Photochemistry, Fluorescence spectroscopy, *Rhizophora stylosa*, *Avicennia marina*, salt-flat





## 1 Introduction

Mangrove ecosystems are widespread established within the intertidal zone along tropical and sub-tropical coastlines (Giri et al., 2011). Although they cover less than 0.5% of the Earth's coastal surface area (Alongi, 2014), mangrove forests play a crucial role in the global carbon cycle by providing several ecosystem services, including carbon fixation and long-term storage in their soils (Kristensen et al., 2008; Donato et al., 2011). These ecosystems account for approximately 10-15% of the carbon sequestered in coastal sediments (Alongi, 2012). However, this carbon stock fluctuates throughout the year due to various factors, such as tidal dynamics, vegetation type, and seasonal variations, which can influence both organic matter (OM) inputs and biogeochemical transformation (Adame et al., 2021; Mouras et al., 2025a).

While humid tropical mangroves have been well studied in this context, (Kathiresan et al., 2013; Sanyal et al., 2020), semi-arid mangroves forest remain less studied. The latter experience low precipitation, large daily temperature fluctuations, low humidity, and high salinity, increasing the physiological stress and reducing primary production. It induces a specific zonation and smaller trees than those in tropical mangroves (Ball, 1998; Leopold et al. 2016; Adame et al., 2021). These conditions can influence their carbon cycling by limiting OM inputs and thus may affect the production and transformation of dissolved organic carbon (DOC), a key component of the carbon pool in mangrove soils. Despite such stressful environments, DOC may still be produced and exported from semi-arid mangrove, contributing to the carbon fluxes with their adjacent ecosystems (Leopold et al., 2017; Jacotot et al., 2018).

In mangrove soils, DOC constitutes a major component of dissolved organic matter (DOM), and originates from different sources, including leaf litter decomposition, roots exudates, and primary producers (Maie et al., 2008; Arnaud et al., 2023; Robin et al., 2024a; Loo et al., 2024). These inputs are transformed through biogeochemical processes, such as leaching and vary according to environmental conditions such as season and hydrology (Alongi et al., 2022). Beyond its origin, DOM plays several ecological roles, it forms complexes with metals (Yamashita and Jaffé, 2008), attenuates UV radiation through chromophoric dissolved organic matter (CDOM) (Arrigo and Brown, 1996; Shank et al., 2010; Zhu et al., 2023), and serves as a food source in the marine microbial loop (Amon and Benner 1994; Chow et al., 2022). Recent finding suggest that DOM quality not only reflects ecosystem processes but also shapes them, indeed, DOM characteristics have been shown to influence benthic microbial communities in tropical coastal systems (Meyneng et al., 2024).

Mangrove ecosystems are now recognized as significant contributors to coastal DOM fluxes (Dittmar et al., 2006; Alongi, 2022; Adame et al., 2024), primarily through the export of DOC (Dittmar et al., 2001; Ray et al., 2021; Cabral et al., 2024), yet quantifying DOC dynamics in mangrove soils remains challenging. It depends on both autochthonous and allochthonous inputs, tidal transport, and biogeochemical drivers that influence both production and export (Shank et al., 2010; Maie et al., 2012; Cawley et al., 2014; Xiao et al., 2023). These mechanisms are well documented in tropical mangrove compared to semi-arid mangroves, where environmental conditions may influence both DOM quantity and quality. Optical techniques such as UV-visible absorbance and excitation emission matrix (EEM) fluorescence spectroscopy combined with parallel factor analysis (PARAFAC) are effective to characterize DOM composition and identify their sources (Coble, 2007; Hansen et al., 2016). Maie et al (2012) used EEM-PARAFAC method to distinguished spatial and seasonal variability of DOM in subtropical wetlands, providing a useful framework that could also be applied to semi-arid mangrove forest. Recently, we showed that DOM fluorescence can be a useful tool to assess OM quality in mangrove soils (Mouras et al., 2025a).

In New Caledonia, a French archipelago in the southwestern Pacific Ocean, the main island stretches 500 km in length and 50 km in width between latitudes 20°S and 23°S and hosts over 35,000 hectares of mangroves, with 88% of this surface developing on the semi-arid west coast of the island (Marchand et al., 2012). These mangrove forests are influenced by a semi-diurnal tidal cycle (Douillet, 2001) and structured along a clear land-sea gradient, with three monospecific zones: the landward salt-flat without vegetation, an intermediate zone dominated by *Avicennia marina*, and a seaward zone occupied by *Rhizophora*



*spp.* (Duke et al., 1998; Marchand et al., 2016). This spatial organization reflects the influence of tidal immersion and porewater salinity on species distribution (Noël et al., 2014). If some aspects of the C cycling were studied in these mangroves (Leopold et al., 2017; Jacotot et al., 2018), few data are available concerning DOM dynamics.

The main objective of this study is to improve understanding of carbon cycling in semi-arid mangroves by assessing how seasonal and spatial variability influence DOM dynamics. We aim to investigate how variations in DOM quantity and quality, shaped by salinity gradients and seasonal conditions, may reflect shifts in OM production, transformation and potential spatial dynamics. To reach our goal, we combined bulk carbon measurements (TOC, DOC) with optical analyses of DOM quality using UV-visible absorbance (CDOM) and fluorescence spectroscopy (FDOM), coupled with PARAFAC modelling. We also determined the mineralogical composition of the soil samples, as mineral phases can influence OM retention. Our sampling strategy was designed to capture both spatial gradients in vegetation cover and tidal exposure by comparing three distinct intertidal habitats: salt-flat, *Avicennia marina* stand, and *Rhizophora stylosa* stand located along the west coast of New Caledonia. We also explored the seasonal variability, by sampling during both the dry and the warm wet seasons. Given the semi-arid conditions and the specific zonation of these habitats, we hypothesize that DOM concentration will be highest in *R. stylosa* stands, where trees experience the lowest salinity stress and the highest OM production. Additionally, we also expect that DOM quality will differ between seasons, with fresher OM during the warm and wet season, due to enhanced productivity, compared to the dry season.

## 2 Material & Methods

### 2.1 Study site

Located on the western coast of New Caledonia, the semi-enclosed mangrove of Bouraké (21.946°S, 165.999°E; Fig. 1) exhibits a typical semi-arid mangrove forest structure (Adame et al., 2021). It consists of three distinct habitats arranged along a land-sea gradient: salt-flats on the landward margin, *Avicennia marina* in the intermediate zone, and *Rhizophora stylosa* stands on the seaward edge. This mangrove spans approximately 2.5 km<sup>2</sup>, with *Rhizophora stylosa* as the dominant species. It is connected to the coastal waters of Pritzbuier Bay through a unique channel, which links two sheltered inlets and a coral reef platform extending from the middle of the channel to the mangrove forest. Bouraké has been studied as a natural laboratory to investigate the responses of marine organisms to extreme environmental conditions (Dubuc et al., 2019; Alessi et al., 2024). However, no studies have specifically focused on the influence of mangrove soils on the biogeochemical processes of this semi-enclosed lagoon.

Geologically, Bouraké is characterized by a volcano-sedimentary substrate (Ullmann et al., 2014) unaffected by external terrigenous sediments and organic inputs, with no direct freshwater input from rivers. Additionally, the presence of coral ecosystem within the sandy sediments of adjacent areas and the mangrove channel enhances its ecological significance by providing nursery habitat for several species including ray-finned fish (Dubuc et al., 2019) while also contributing to sediment stabilization.

Three sampling zones were selected along a land-sea gradient, each featuring a specific habitat, to investigate the influence of mangrove habitat and seasons on the composition and dynamics of OM. The first site landward is labelled “salt-flat” for zone covered by no vegetation. The second site named “*A. marina*” consist of monospecific stand of *Avicennia marina* forest. The third site seaward, “*R. stylosa*” consist of monospecific stand of *Rhizophora stylosa* mangrove (Fig.1).

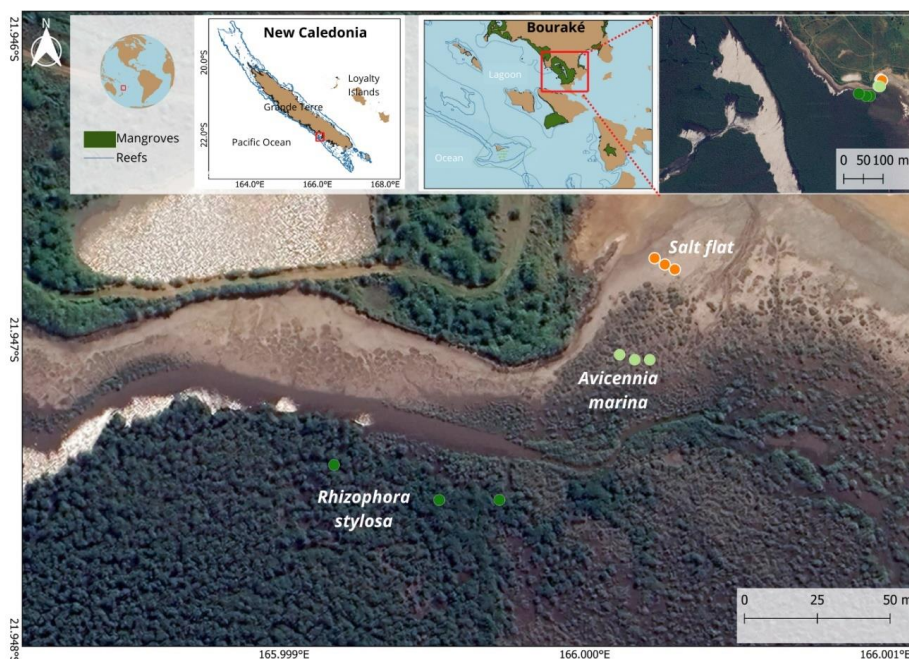


**Figure 1 : Map of Bouraké mangrove land-sea gradient, New Caledonia. The nine soil cores sampled in June and October 2023 are indicated by dots. (QGIS 3.28.6, © Google earth™, December 2024).**

## 2.2 Field sampling

Field sampling was conducted at low tide at the end of two seasons: for the wet season (June 19, 2023) with a total precipitation over the 5 months before of 356 mm and for the dry season (October 26, 2023) with a total precipitation of 269 mm for the last 5 months before sampling (météo France). At each site, three replicates of 30 cm depth-long soil cores were collected using a manual corer. Each core was then sectioned into three 10 cm layers (0-10 cm, 10-20 cm, 20-30 cm) using a Teflon spatula.

Physicochemical parameters, including temperature, pH and redox potential (Eh), were measured *in situ* directly in the soil core at the center of each section (5, 15, 25 cm). pH was recorded with a 3320 WTW® SenTix® 81 glass electrode, calibrated prior to use with buffer solutions (pH 4, pH 7, pH 10). Redox potential was determined using a SenTix® ORP WTW® pH315i electrode checked daily with a 220-mV standard solution. To obtain Eh values relative to the standard hydrogen electrode (SHE), a correction factor of +220 mV was added to the measured values, as recommended for Ag/AgCl reference electrodes.

Porewater was extracted *in situ* from each section using Rhizon® MOM-10 cm soil moisture samplers (0.2 µm pore size) inserted into the entire soil sections. This sampling method ensured that the porewater collected was representative of each 10 cm-thick soil layers. A 10 mL pressurized syringe was connected for extraction, and a drop of porewater was used to measure salinity with a refractometer (ATC). Porewater were then filtered through pre-combusted (450°C, 4h) 25 mm glass fiber filters (Whatman GFF, 0.7 µm) for analyses, including DOC, CDOM, and FDOM. Solid samples were collected from each soil section using a cylindrical syringe and immediately stored in a cooler for subsequent laboratory analysis of TOC and sediment properties.



Samples were transported in coolers to the laboratory and stored under appropriate conditions for further analysis. For DOC analysis, samples were acidified (HCl, pH < 2) and stored in pre-cleaned 24 mL glass vials (Wheaton) with Teflon/silicone septa, in the dark at 4°C. For DOM analysis, porewater were stored in glass vials that had been previously  
 130 cleaned with 10% HCl, rinsed three times with Milli-Q water, and combusted (450 °C, 6 h) before being stored at 4 °C in the dark. Solid soils samples were kept at −20 °C. Frozen soil samples were lyophilized 48 h (Alpha 1-2 LDplus - CHRIST).

## 2.3 Analytical methods

### 2.3.1 Soil grain size

For soil samples with an OM content exceeding 5%, a pretreatment step was applied to remove OM before analysis  
 135 (Gee & Bauder, 1996). Under a fume hood, 20 g of dried sample was placed in a 500 mL beaker, followed by the addition of 5 mL of hydrogen peroxide (H<sub>2</sub>O<sub>2</sub>) and 2 mL of acetic acid (CH<sub>3</sub>COOH). The beakers were then heated on a hot plate at 40°C, and up to 20 mL of H<sub>2</sub>O<sub>2</sub> was gradually added per beaker until the reactions were complete. After evaporation, the samples were resuspended in ultrapure water in 15 mL conical vials. Particle size distribution was then measured using a laser diffraction granulometer (MASTERSIZER HYDRO 2000S, MALVERN).

### 140 2.3.2 Soil mineralogy by X-Ray Diffraction (XRD)

Prior to analysis, samples were lyophilized 48h, then ground with a planetary agate mortar to obtain homogeneous powders <100 µm. A single core was selected from each habitat during the wet season. For each core, three section depths were analysed (0-10, 10-20, and 20-30 cm), resulting in a total of nine samples. The mangrove soils' mineralogical composition was determined by X-Ray Diffraction (XRD) using a PANalytical AERIS XRD Diffractometer with a Co source, operated at  
 145 40 kV and 15 mA. The diffractometer was equipped with an iron beta-filter, 0.04 Sollers slits and a ¼ divergent slit. Measurements were performed between 3 to 90°2θ with a step size of 0,003 and an acquisition time of 59s. All XRD were normalised using the intensity of the 3.34 angström quartz peak in order to compare the evolution of mineral proportion to the quartz content. Phase identification was based on diffraction peak matching with standard mineral databases using the Xpert™ software.

### 150 2.3.3 Bulk density

Sediment bulk density was determined using a volumetric sampling method. Fresh sediment was collected in a 20 cm<sup>3</sup> cylindrical syringe, ensuring minimal compaction. The wet sample was weighed immediately to determine its initial mass. It was then freeze-dried to remove all moisture before being weighed again to obtain the dry sediment mass. The water content was calculated as the difference between the wet and dry masses. Bulk density (g.cm<sup>-3</sup>) was then determined as the ratio of the  
 155 dry sediment mass to the initial sample volume.

### 2.3.4 Total and dissolved organic carbon (TOC & DOC)

TOC and DOC concentrations were measured using a Shimadzu TOC-VCSH carbon analyser, which operates on high-temperature catalytic oxidation with infrared detection and is equipped with an auto-sampler. Blanks and standard solutions were analysed every 10 samples to ensure quality control, with all replicates maintaining an error margin below 10%.  
 160 Each sample was analysed in triplicate to guarantee precision. For TOC analysis, the same dried and grounded samples prepared for XRD were used. Measurements were performed in triplicate using a Shimadzu SSM-5000A solid sample module, based on high-temperature catalytic combustion. Each sample was covered with ceramic fiber prior to analysis. Calibration and quality control was ensured by regular measurements of internal reference materials and a glucose 40% standard.





### 2.3.5 Chromophoric dissolved organic matter (CDOM)

CDOM absorption spectra were measured every nanometer from 200 to 700 nm using a Shimadzu UV-1700® spectrophotometer and 1 cm quartz cuvette. Spectral absorption coefficients ( $m^{-1}$ ) and indicators were calculated to characterize the DOM after subtracting the raw absorbance of blank prepared with Milli-Q water, using the method of Yamashita and Tanoue (2009). The spectral slopes ( $S_{275-295}$  and  $S_{350-400}$ ) were calculated to differentiate CDOM sources, allowing distinction between marine and terrestrial inputs (Hansen et al., 2016). The  $S_R$  ratio, obtained from the ratio of these two slopes, was used to assess CDOM molecular weight and its susceptibility to photodegradation (Helms et al., 2008; Hansen et al., 2016). Additionally, the  $E_2/E_3$  index was used as an indicator of aromaticity and molecular weight (Rocha et al., 1999; Hautala et al., 2000). The SUVA a proxy for aromaticity and humification is calculated as the ratio of absorbance at 254 nm to the concentration of DOC.

### 2.3.6 Fluorescent dissolved organic matter (FDOM)

Fluorescence analyses were performed in quartz cell with a 2 mm optical path length (Hellma ®) using a PERKIN ELMER LS 55 spectrofluorometer. Excitation-Emission matrices (EEMs) (Coble, 1996, 2007) were obtained for emission wavelengths from 280 to 550 nm (5 nm steps) and excitation wavelengths from 200 to 500 nm (5 nm steps). The excitation and emission slit widths were both set to 10 nm. Before each analysis, the cell was rinsed with 10% HCl, Milli-Q water, and the sample itself.

The EEM data were processed using Parallel Factor Analysis (PARAFAC) to identify the main fluorophore groups (Bro, 1997). PARAFAC analysis was conducted with the ProgMEEF software (Mediterranean Institute of Oceanography (MIO) - University of Toulon, 2022) through the MATLAB R2017a platform. Prior to interpretation, the EEMs were normalized to remove the influence of Raman and Rayleigh scattering bands by dividing the EEMs by the Raman scattering peak of pure water at Ex/Em = 275/303 nm (Coble, 1996). The Raman standardization was carried out following the method described by Zepp et al. (2004). Fluorescence intensities were converted to Quinine Sulfate Units (QSU) using a calibration curve based on quinine sulfate in 0.1 N  $H_2SO_4$ , measured at Ex/Em = 350/450 nm (Coble, 1996). The EEMs were then decomposed using the CORCONDIA (CORE CONSistency DIAGnostic) algorithm to identify the primary fluorophore groups. This algorithm calculates a percentage value, with components exceeding 60% considered optimal (Zhao, 2011). The identified components were compared with existing literature using the Openfluor database (Murphy et al., 2014). The relative abundance of each fluorescent component (C%) was determined as ratio of its fluorescence intensity to the total fluorescence intensity of all components, as described by Santín et al. (2009).

The humification index (HIX) was calculated using the methods of McKnight et al. (2001). HIX values ranged from 0 to 1, with higher values reflecting a greater degree of humification. The biological index (BIX) was calculated using the methods of Parlanti et al. (2000). A high BIX value ( $>1$ ) indicates a dominant autochthonous DOM source, while lower value indicates low level of autochthonous production (Huguet et al., 2009).

## 2.4 Statistics

Statistical analyses were conducted using R software (v.4.0.3). Descriptive statistics were first applied to summarize the dataset. Normality and homoscedasticity of the data were assessed using Shapiro-Wilk and Levene's tests, respectively. For parametric data, one-way ANOVA was performed to test differences among groups, followed by Tukey's post-hoc test when significant differences were detected. When assumptions of normality and homogeneity were not met, the Kruskal-Wallis non-parametric test was used instead, with Wilcoxon pairwise comparisons for post-hoc analysis. To assess differences



between the dry and wet seasons, Student's t-test was applied for parametric, and the Mann-Whitney U test was used for non-parametric data.

To analyse the effects of season, mangrove habitat type, and sediment depth on the overall environmental dataset including physicochemical parameters (salinity, pH, Eh, temperature, water content, granulometry, density) as well as carbon-related variables (TOC, DOC, CDOM, FDOM), a PERMANOVA (Permutational Multivariate Analysis of Variance) was conducted using the `adonis2` function from the R `vegan` package. The analysis was based on Bray-Curtis dissimilarities calculated from fourth-root transformed data, with 999 permutations. Pairwise comparisons were performed when significant effects were detected. A non-metric multidimensional scaling (NMDS) was performed using the `metaMDS` function from the `vegan` R package, based on Bray-Curtis dissimilarities calculated from fourth-root transformed data. The ordination was constrained to two dimensions ( $k = 2$ ), and the quality of the representation was assessed using the stress value. Statistical significance was set at  $p < 0.05$  for all analyses.

### 3 Results

#### 3.1 Factor weight analysis

The PERMANOVA revealed that habitat type (salt-flat, *A. marina* and *R. stylosa*) had the strongest effect on sample differentiation ( $R^2 = 63.1\%$ ,  $p = 0.001$ ), followed by season (Dry and Wet) ( $R^2 = 4.8\%$ ,  $p = 0.004$ ). In contrast, soil depth (0-10, 10-20, 20-30 cm) had a negligible effect ( $R^2 = 2.4\%$ ,  $p = 0.1$ ), indicating that the vertical stratification of soils properties was less pronounced compared to the spatial (habitat) and temporal (seasonal) effects (Table A1).

A non-metric multidimensional scaling (nMDS) plot (stress = 0.09) confirms that habitat type is the primary structuring factor, particularly differentiating salt-flat from both *A. marina* and *R. stylosa* along nMDS axis 1 (Figure A3). Seasonal effects are also visible, especially for salt-flat, where two distinct clusters separate the dry and wet seasons. A similar trend is observed for *A. marina*, whereas *R. stylosa* does not show clear seasonal clustering.

Principal Component Analysis (PCA) results (Fig. 2) show a clear separation of samples according to the intertidal gradient. The first principal component (PC1) explains 39.9% of the variance, captures the contrast between land-derived OM (C1), dominant in the salt-flat, and mangrove-derived OM (C2), which increases seaward. The second component (PC2), explaining 22% of the variance, captures additional variation related to fluorescence indices such as biological activity index (BIX).

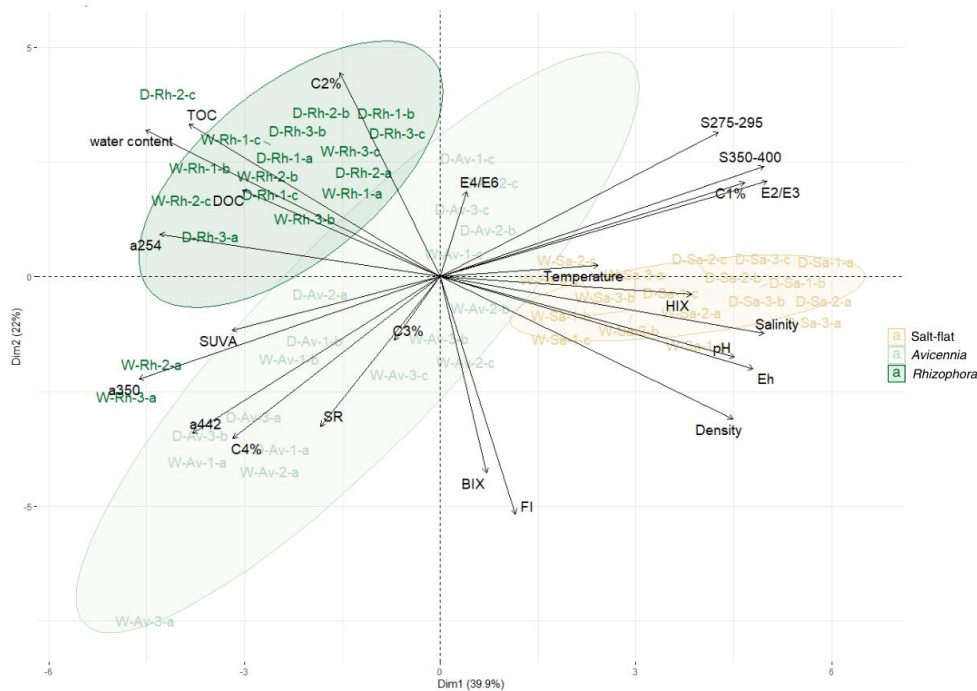


**Figure 2 : Biplot of principal component analysis (PCA) (Dim 1: 39.9%, Dim 2: 22%) with K-means Clustering (K = 3)**

Although soil depth does not have a significant influence in the multivariate analysis, it may affect specific parameters at a finer scale. However, given its limited contribution to the sample differentiation compared to habitat type and season, depth is not represented in this study. The focus was on the most influential factors, such as habitat zonation and seasonal variability.

**3.2 Soil characteristics**

Across the three mangrove habitats along the intertidal gradient, the soils show variation in their mineralogical composition. Granulometric analysis indicated no major differences related to habitat, although silt content was slightly higher in *R. stylosa* soils compared to salt-flat and *A. marina* (Table A2). XRD patterns (Fig. 3) revealed mineralogical differences between mangrove habitat. Quartz (SiO<sub>2</sub>) dominated in salt-flat and *A. marina* soils, whereas *R. stylosa* soils showed lower quartz intensity and higher feldspar content, particularly in surface layers. In parallel, sulfur-bearing minerals such as jarosite (sulfates; KFe<sub>3</sub>(OH)<sub>6</sub>(SO<sub>4</sub>)<sub>2</sub>), anhydrite (sulfate; CaSO<sub>4</sub>), and pyrite (FeS<sub>2</sub>, sulfide) were identified in *R. stylosa* soils. Samples from this tree-species display pronounced peaks for these minerals, demonstrating their non-negligible content compare to quartz. However, small poorly intense and broad peaks linked to anhydrite (with diagnostic peaks (d.p.) around 3.5 Å), Ti-oxides (d.p. 3.26 Å), pyrite (d.p. 3.1 Å/2.43 Å) and hematite (d.p. 3.68 Å, Fe<sub>2</sub>O<sub>3</sub>) could also be identified in other samples (Salt Marsh and Avicennia), but their content is definitively lower than for the *R. stylosa* samples. Small content of goethite (Fe-oxyhydroxie, FeOOH) is also likely present (broad d.p. at 4.19 Å) in the *R. stylosa* substrate.



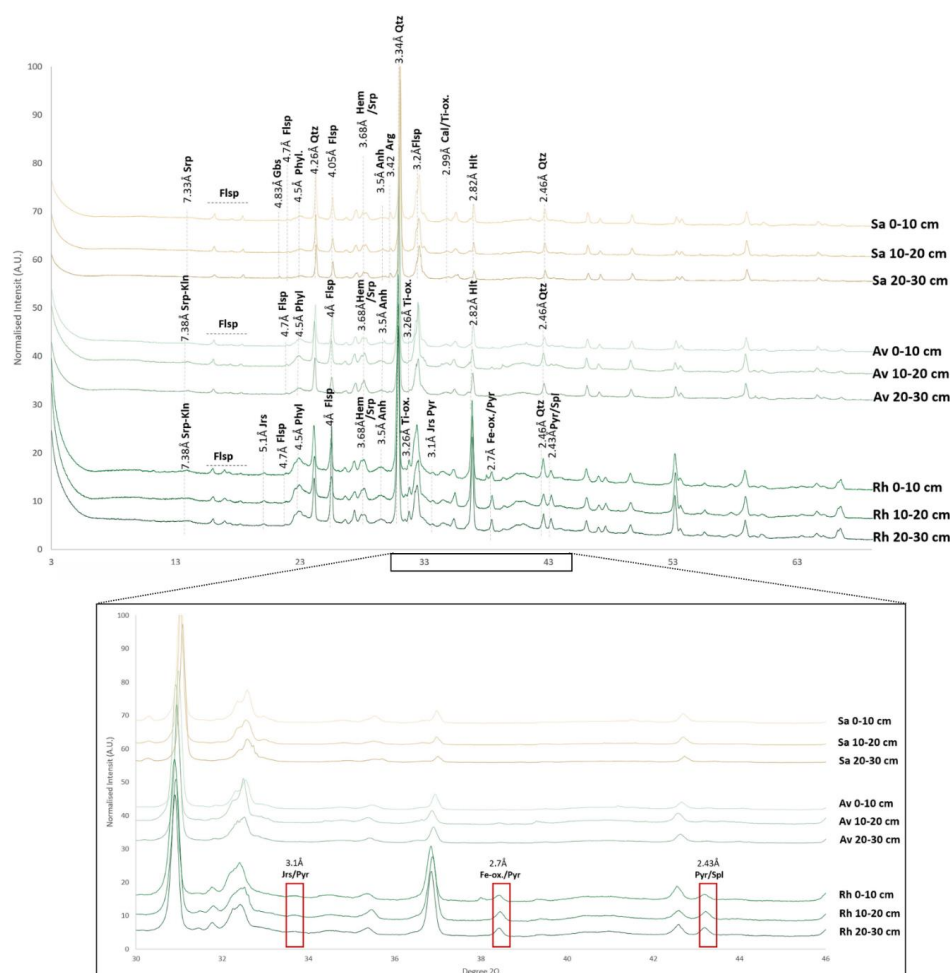


**Figure 3 : X-ray diffraction (XRD) patterns of soil samples collected from Salt-flat (Sa), *Avicennia marina* (Av), and *Rhizophora stylosa* (Rh) stands. Major identified mineral phases include: Srp: Serpentine, Kln: Kaolinite, Flsp: feldspar, Jrs: jarosite, Gbs: gibbsite, Phyl: phyllosilicates, Qtz: quartz, Hem: hematite, Anh: anhydrite, Arg: aragonite, Ti-Ox: titanium oxides, Pyr: pyrite, Cal: Calcite (Mg), Hlt: halite, Fe-ox: iron oxides and oxyhydroxides (grouped).**

### 3.3 Physico-chemical parameters

Soil salinity exhibited significant differences among the three habitats ( $p < 0.05$ ), with the highest values recorded in the salt-flat, followed by the *A. marina* and *R. stylosa* stands (Fig. 4). A significant effect of season was also measured. Salinity was significantly higher during the dry season compared to the wet season in both the salt-flat ( $117.4 \pm 28.5$  vs.  $88.1 \pm 15.5$ ), and slightly higher in the *R. stylosa* site ( $47 \pm 2.1$  vs.  $44.8 \pm 1.7$ ;  $p < 0.05$ ). In contrast, no seasonal variation was observed in the *A. marina* stand, where values remained stable between seasons ( $55.5 \pm 3.04$  vs.  $56.7 \pm 2.58$ ;  $p > 0.05$ ).

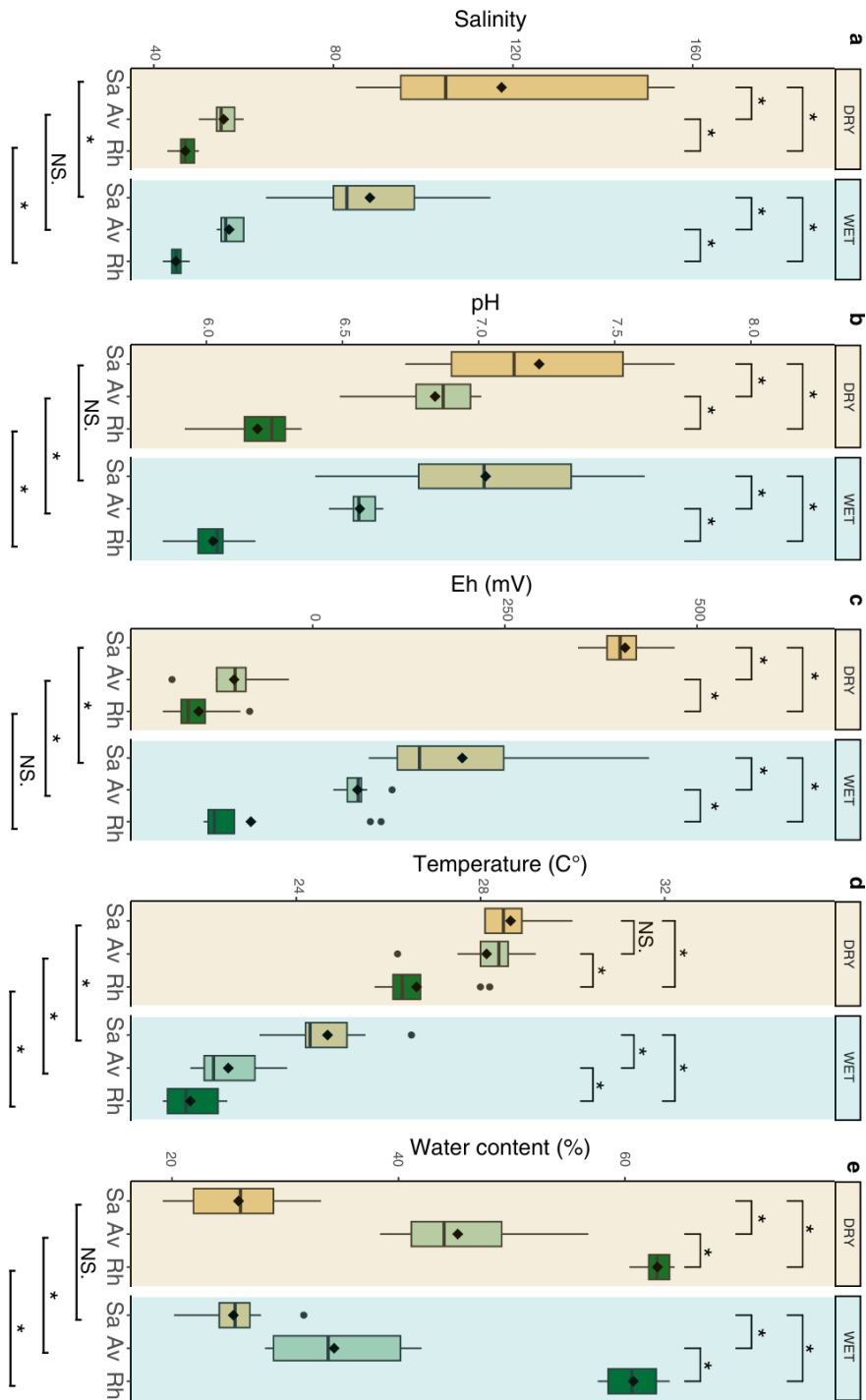
Soil water content followed an opposite trend to salinity, with significantly higher values in *R. stylosa* stands, intermediate levels in *A. marina*, and the lowest percentages in the salt-flat ( $p < 0.05$ ). Seasonal variations were habitat-dependent: a slight decrease was observed in *R. stylosa* soils ( $62.9 \pm 1.2\%$  during the dry season vs.  $60.7 \pm 2.4\%$  during the wet season, Student's t-test,  $p < 0.05$ ), while *A. marina* exhibited a more pronounced decrease ( $45.2 \pm 6.1\%$  vs.  $34.3 \pm 5.5\%$ , Student's t-test,  $p < 0.05$ ). In contrast, no significant seasonal variation was detected in the salt-flat ( $25.8 \pm 5.1\%$  vs.  $25.4 \pm 3.5\%$ , Student's t-test,  $p > 0.05$ ).



Redox potential (Eh) exhibited clear spatial differences along the intertidal gradient ( $p < 0.05$ ), with the most positives values recorded in the salt-flat, intermediate values in the *A. marina* stand, and the most negative values measured under *R. stylosa*. Seasonal patterns also emerged, but differed between habitats. In the salt-flat, Eh values were significantly higher during the dry season ( $406 \pm 40$  mV) compared to the wet season ( $194 \pm 136$  mV). In contrast, in both *A. marina* and *R. stylosa* stands, values were significantly lower during the dry season (*A. marina*:  $-102 \pm 43$  mV vs.  $58 \pm 21$  mV; *R. stylosa*:  $-148 \pm 38$  mV vs.  $-80 \pm 93$  mV;  $p < 0.05$ ).

Soil acidity varied significantly between habitats, with *R. stylosa* stands being the most acidic ( $p < 0.05$ ) (Fig.3; Table A3). Mean pH values were lower in *R. stylosa* ( $6.02 \pm 0.1$  in the wet season vs.  $6.18 \pm 0.1$  in the dry season) compared to *A. marina* ( $6.56 \pm 0.06$  vs.  $6.84 \pm 0.1$ ) and salt-flat soils ( $7.02 \pm 0.4$  vs.  $7.22 \pm 0.3$ ). A significant seasonal variation was observed in *R. stylosa* and *A. marina* stands, with lower pH values recorded during the wet season ( $p < 0.05$ ). In contrast, no seasonal pH difference was detected in salt-flat soils.

Soil temperature varied significantly between habitats, with the highest values measured in the salt-flat, intermediates values in the *A. marina* stands, and lowest in the *R. stylosa* stands ( $p < 0.05$ ) whatever the season. During the dry season, temperatures were similar in salt-flat and *A. marina* soils (both around  $28^\circ\text{C}$ ), whereas *R. stylosa* remained significantly cooler ( $26.6 \pm 0.8^\circ\text{C}$ ,  $p < 0.05$ ). In the wet season, temperatures dropped across all sites, ranging from  $24.6 \pm 0.9^\circ\text{C}$  in the salt-flat to  $21.7 \pm 0.5^\circ\text{C}$  in the *R. stylosa* zone ( $p < 0.05$ ).



280 **Figure 4 : Seasonal and spatial variations of physico-chemical parameters (salinity, pH, Eh, temperature, and water content) in salt-flat (Sa), *Avicennia marina* (Av), and *Rhizophora stylosa* (Rh). Significant differences between habitats (ANOVA/Kruskal-Wallis, see Table A8 for full test results) and between seasons (Student's t-test/Mann-Whitney, see Table A7 for full test results) are indicated by \*  $p < 0.05$ , NS = no significant difference.**



### 3.4 Spatio-temporal distribution of organic carbon (TOC, DOC and CDOM)

285 TOC concentrations in soils differed significantly between habitats ( $p < 0.05$ ), with the highest concentration measured in the *R. stylosa* stand, followed by *A. marina* and the salt-flat. In *R. stylosa* soils, TOC levels remained consistently high whatever the season (8.3-10.4% during the wet season vs. 8.7-10.1% during the dry season;  $p > 0.05$ ). In contrast, significant seasonal variations were observed in *A. marina* and salt-flat soils ( $p < 0.05$ ), with higher TOC concentrations during the dry season. TOC increased from 0.6-0.7% (wet) to 1.9-2.0% (dry) in salt-flat soils, and from 1.2-2.2% to 2.8-4.5% in *A. marina* soils.

Along the land-to-sea gradient, TOC content increased significantly from the landward salt-flat to the seaward *R. stylosa* stand at both seasons ( $p < 0.05$ ; Fig. 5, Table A2). This pattern was reflected in the Spearman correlation matrix (Fig. A1), which revealed significant negative correlations between TOC and key physicochemical parameters, including pH ( $\rho = -0.76$ ), redox potential (Eh;  $\rho = -0.63$ ), and salinity ( $\rho = -0.59$ ).

295 DOC concentrations showed a clear spatial pattern along the land-sea gradient, with increasing values from the salt-flat to the *R. stylosa* stand, particularly during the dry season (Fig. 5). Although a similar trend was observed during the wet season, the differences between habitats were not statistically significant. Seasonal variations in DOC concentrations were habitat-dependent. At the salt-flat and *A. marina* sites, DOC levels were significantly higher during the wet season, increasing from  $12 \pm 2 \text{ mg} \cdot \text{L}^{-1}$  to  $17 \pm 2 \text{ mg} \cdot \text{L}^{-1}$  in the salt-flat soils, and from  $22 \pm 9 \text{ mg} \cdot \text{L}^{-1}$  to  $38 \pm 18 \text{ mg} \cdot \text{L}^{-1}$  under *A. marina* ( $p < 0.05$ ). In contrast, no significant seasonal change was detected in *R. stylosa* soils, where DOC concentrations remained relatively stable across seasons ( $53 \pm 31 \text{ mg} \cdot \text{L}^{-1}$  during the dry season vs.  $45 \pm 32 \text{ mg} \cdot \text{L}^{-1}$  during the wet season;  $p > 0.05$ ).

300 According to the Spearman correlation matrix (Fig. A1), DOC concentrations were negatively correlated with pH ( $\rho = -0.45$ ), redox potential (Eh;  $\rho = -0.44$ ), salinity ( $\rho = -0.46$ ), and temperature ( $\rho = -0.28$ ), all significant at  $p < 0.05$ .

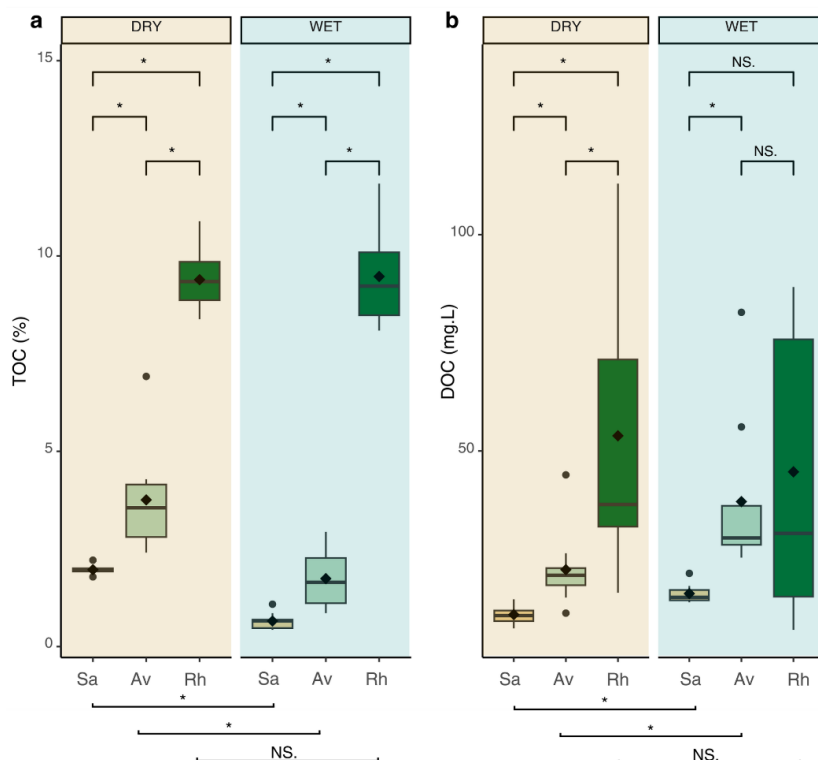
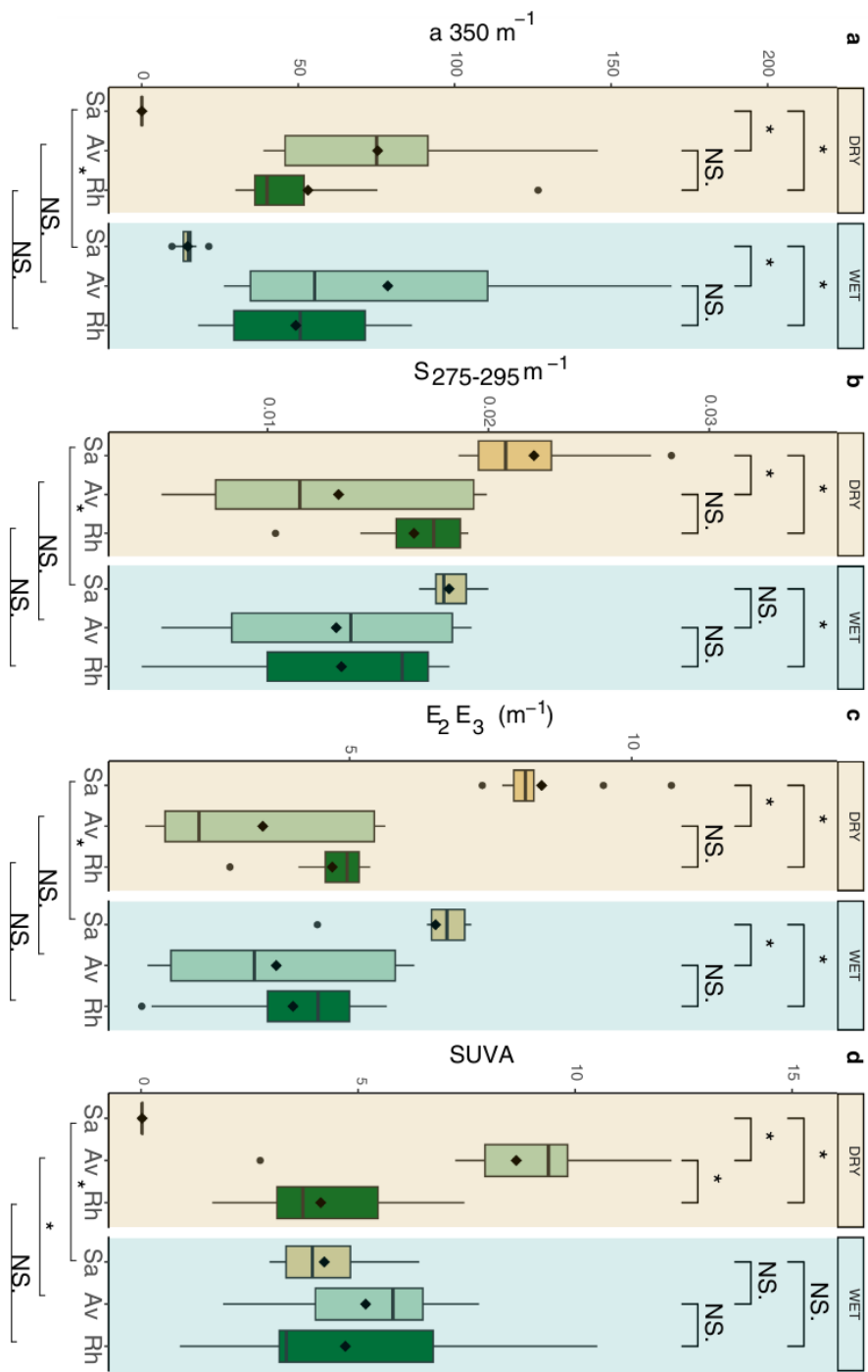


**Figure 5 : Seasonal and spatial variations of TOC (%) and DOC concentrations (mg. L<sup>-1</sup>) across a land-sea gradient in salt-flat (Sa), *Avicennia marina* (Av), and *Rhizophora stylosa* (Rh). Significant differences between habitats (ANOVA/Kruskal-Wallis, see Table A8 for full test results) and between seasons (Student's t-test/Mann-Whitney) are indicated (\*  $p < 0.05$ , NS = no significant difference, see Table A7 for full test results).**

CDOM optical properties, represented by absorption at 350 nm ( $a_{350}$ ), spectral slope ( $S_{275-295}$ ), and the  $E_2/E_3$  ratio (Fig. 6; Table A4), varied significantly along the intertidal gradient. CDOM levels ( $a_{350}$ ) were lowest in the salt-flat, intermediate in *A. marina*, and highest in *R. stylosa* soils. In contrast,  $S_{275-295}$  and  $E_2/E_3$  values followed the opposite trend, being highest in the salt-flat and lowest in *R. stylosa*, reflecting differences in DOM composition and degradation status across habitats. SUVA values also differed significantly between habitats, with the highest values in *A. marina* soils and the lowest in the salt-flat ( $p < 0.05$ ).

Seasonal variations in CDOM characteristics were most pronounced in the salt-flat. There,  $a_{350}$  increased significantly during the wet season ( $14.6 \pm 3.6$ ) compared to the dry season ( $0.05 \pm 0.02$ ;  $p < 0.05$ ), while  $S_{275-295}$  and  $E_2/E_3$  values were significantly lower during the wet season ( $18.2 \pm 1.0$  and  $6.5 \pm 0.8$ ) than in the dry season ( $22.1 \pm 3.5$  and  $8.4 \pm 1.0$ ;  $p < 0.05$ ). SUVA in the salt-flat followed this trend, increasing from  $0.02 \pm 0.0$  to  $4.2 \pm 1.0$  ( $p < 0.05$ ). In *A. marina* soils, seasonal variations were also significant for SUVA, which decreased from  $8.6 \pm 2.6$  in the dry season to  $5.1 \pm 1.8$  in the wet season ( $p < 0.05$ ). However, no significant seasonal changes were detected for  $a_{350}$ ,  $S_{275-295}$ , or  $E_2/E_3$  ( $p > 0.05$ ). *R. stylosa* stands exhibited no significant seasonal differences in any CDOM parameter, with stable values suggesting a relatively consistent DOM composition throughout the year.



325 **Figure 6 : Seasonal and spatial variations of CDOM indicators ( $a_{350}$ ,  $S_{275-295}$ ,  $E_2/E_3$ , and SUVA) across a land-sea gradient in Salt-flat (Sa), *Avicennia marina* (Av), and *Rhizophora stylosa* (Rh). Significant differences between habitats (ANOVA/Kruskal-Wallis, see Table A8 for full test results) and between seasons (Student's t-test/Mann-Whitney) are indicated (\*  $p < 0.05$ , NS = no significant difference, see Table A7 for full test results).**





### 3.5 Spatio-temporal distribution of FDOM components

Across the three mangrove habitats and for both season, four fluorescent components (C1-C4) were validated by  
 330 PARAFAC analysis, using 54 EEMs from soil porewater. The four-contour plots and relative fluorescence abundance (%) are  
 represented in Fig. 6 and Fig. A2, while their concentrations in QSU (Quinine Sulfate Units) are provided in Tab. A6. They  
 were compared with the literature and the OpenFluor database (Murphy et al., 2014), all component showed significant  
 matches (Tucker's correlation coefficient > 0.95) (Tab. A5). C1 and C2 correspond to terrestrial humic-like substances, with  
 excitation peaks at 250(330) nm and 215(280, 380) nm, and emission maxima at 431 nm and 484 nm, respectively. C3 exhibits  
 335 two excitation peaks (230 nm, 300 nm) and an emission at 387 nm, similar to marine humic-like fluorescence. C4 is  
 characterized by an excitation peak below 200 nm and an emission at 469 nm, consistent with photodegradation-derived humic-  
 like substances, as previously reported by Lambert et al. (2016) and Amaral et al. (2020).

In terms of spatial variation, the relative abundance of C1 was significantly higher in the salt-flat habitat compared to  
 the two mangrove stands (*A. marina* and *R. stylosa*) during both seasons ( $p < 0.05$ ). No significant difference in C1 relative  
 340 abundance was observed between *A. marina* and *R. stylosa* whatever the season. In contrast, C2 followed a different pattern,  
 with its highest abundance in the *R. stylosa* habitat for both seasons. During the dry season, the salt-flat exhibited significantly  
 lowest C2 abundance than the other two habitats ( $p < 0.05$ ). C3 showed no significant differences across habitats during the  
 dry season., but its relative abundance increased significantly in *A. marina* during the wet season. C4 did not show any  
 significant spatial variations across habitats in either season.

345 Regarding seasonal variations (Fig. 7), in the salt-flat habitat, C1 % was significantly higher during the dry season ( $p$   
 $< 0.05$ ), while C4 showed the opposite pattern with higher values during the wet season. C2 and C3 did not vary significantly  
 between seasons in this habitat. In the *A. marina* stand, both C1% and C2% were significantly more abundant during the dry  
 season, while C3 increased significantly during the wet season. C4 remained stable across seasons. In the *R. stylosa* stand, no  
 significant seasonal differences were observed for any of the four components.

350 Figure 8 presents boxplots of the Humification Index (HIX) and the Biological Index (BIX) across the mangrove land-  
 sea gradient. For BIX, significant spatial differences were observed in both seasons. During the dry season, biological activity  
 was highest in the salt-flats, followed by *A. marina*, and lowest in *R. stylosa*, following the land-to-sea gradient. In the wet  
 season, the highest BIX values were found in *A. marina* stands ( $0.8 \pm 0.1$ ), followed by the salt-flats ( $0.6 \pm 0.03$ ) and *R. stylosa*  
 ( $0.5 \pm 0.08$ ). For HIX, during the dry season, values in *A. marina* ( $32 \pm 13$ ) and salt-flat habitats ( $30 \pm 9.6$ ) were similar and  
 355 significantly higher than those measured in *R. stylosa* ( $9.3 \pm 6.0$ ). A similar pattern was observed in the wet season, with the  
 salt-flat remaining the most humified site ( $29 \pm 4.5$ ), while *A. marina* and *R. stylosa* showed lower and comparable HIX values.

Regarding seasonal variation, in the salt-flat, both indices remained stable across seasons (BIX, dry and wet:  $0.6 \pm 0.03$ ;  
 HIX, dry:  $30 \pm 9.6$  and wet:  $29 \pm 4.5$ ). In the *A. marina* stand, BIX increased significantly in the wet season ( $0.8 \pm 0.1$ )  
 compared to the dry season ( $0.5 \pm 0.06$ ) ( $p$ -value  $< 0.05$ ), while HIX was significantly higher during the dry season ( $32 \pm 13$ )  
 360 than in the wet ( $12 \pm 5.3$ ). In the *R. stylosa* stand, BIX also increased slightly during the wet season ( $0.5 \pm 0.08$  vs.  $0.4 \pm 0.04$ ),  
 while HIX followed the opposite trend (dry:  $9.3 \pm 6.0$ ; wet:  $5.8 \pm 4.4$ ).

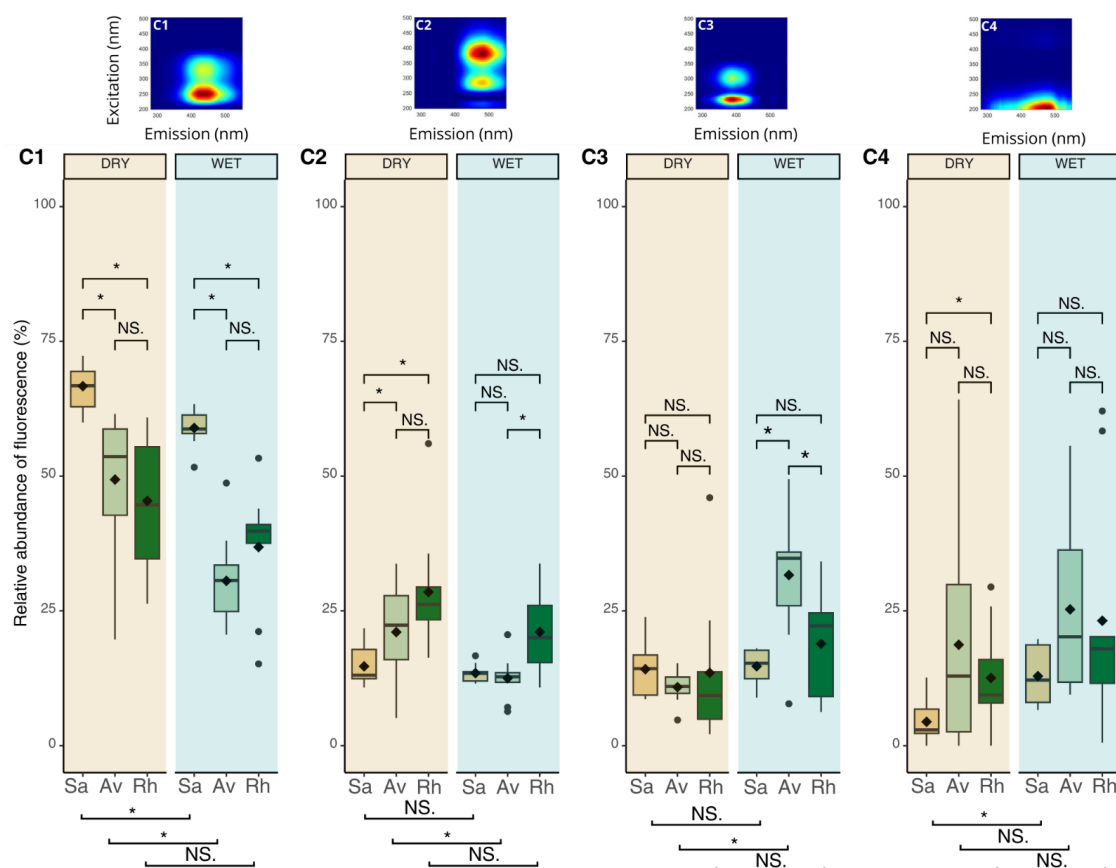
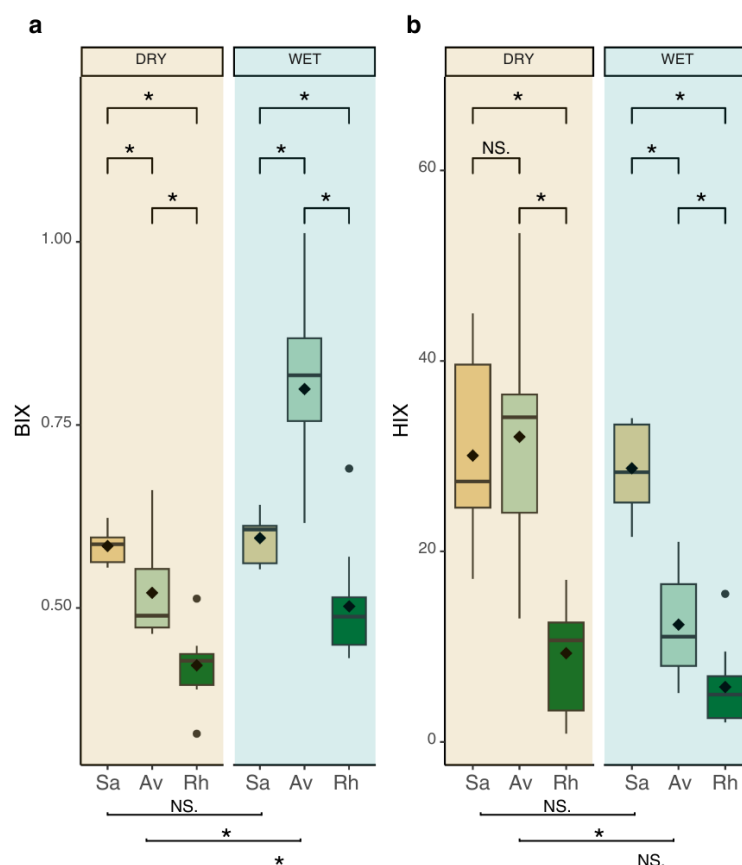


Figure 7 : EEM contour plots of the four PARAFAC components (C1, C2, C3, C4) and seasonal variations in their relative fluorescence abundance (%) across a land-sea gradient in (salt-flat (Sa), *Avicennia marina* (Av), and *Rhizophora stylosa* (Rh). Significant differences between habitats (ANOVA/Kruskal-Wallis, see Table A8 for full test results) and between seasons (Student's t-test/Mann-Whitney) are indicated (\*  $p < 0.05$ , NS = no significant difference, see Table A7 for full test results).



**Figure 8 : Seasonal and spatial variations of the Biological Index (BIX) and Humification Index (HIX) across salt-flat (Sa), *Avicennia marina* (Av), and *Rhizophora stylosa* (Rh). Significant differences between habitats (ANOVA/Kruskal-Wallis, see Table A8 for full test results) and between seasons (Student's t-test/Mann-Whitney) are indicated (\*  $p < 0.05$ , NS = no significant difference, see Table A7 for full test results).**

## 4 Discussion

The results of this study reveal that DOM dynamics in the studied mangrove soils are primarily driven by two connected factors: i) the spatial zonation along the intertidal gradient, and ii) the seasonal variability between the dry and wet seasons. These patterns emerged across both DOM concentration and quality indicators. Therefore, the discussion is structured in two main parts: the first examines the spatial differences in DOM characteristics across the three intertidal habitats, while the second explores how seasonal shifts modulate DOM composition within each zone.

### 4.1 Influence of mangrove zonation on the quality and quantity of DOM in soil porewater

In semi-arid climate, topography, inundation frequency, and evaporation influence mangrove distribution in the intertidal zone, leading to distinct biogeochemical conditions across habitats (Baltzer, 1982; Marchand et al., 2011; Adame et al., 2021).

The salt-flat, which lacks vegetation, is the most exposed to evaporation and to intense solar radiation (Baltzer et al., 1982; Deborde et al., 2015), which contributes to its extreme soil salinity (> 80 ‰, Fig. 4). The presence of desiccation cracks further enhances oxygen penetration, resulting in the highest redox potential (Eh) recorded across our study sites, as observed



385 in other mangroves of the west coast of New Caledonia (Noël et al., 2014). Positive correlations between salinity, pH and Eh  
 (Fig. A1), and their negative relationship with water content, indicate that porewater characteristics are mainly driven by  
 hydroperiods (Marchand et al., 2011; Kristensen et al., 2017). As a result, this habitat exhibited the lowest OM concentrations  
 both in the solid and the dissolved phases and a distinctive highly degraded DOM signature. Optical indicators (low CDOM  
 ( $a_{350}$ ), low SUVA, and high  $S_{275-295}$  and  $E_2/E_3$  value (Fig. 6) suggest a DOM pool of low molecular weight, strongly influenced  
 390 by photo or/and microbial degradations (Helms et al., 2008; Gonsior et al., 2013). Despite low OM content, the salt-flat  
 exhibited a relatively high proportion of one fluorescent DOM component (C1%), classified as terrestrial humic-like (Table  
 A5), typically resulting from degraded vascular and non-vascular plant material (Kida et al., 2021). While its origin remains  
 uncertain, it could partly derive from terrestrial inputs, potentially sourced from the herbaceous vegetation developing in the  
 bay catchment (Hoff et al., 1983) which is dominated by *Poaceae* (*Heteropogon*) and some *Fabaceae* (*Leucaena*  
 395 *leucocephala*). However, given the strong photodegradation at the soil surface in the salt-flat, it is also possible that C1  
 originates from highly altered mangrove-derived material, such as *R. stylosa* or *A. marina* litterfall, transported at flood tide  
 and further transformed under the conditions of this habitat. Thus, the complex DOM pool likely reflects a potential  
 combination of terrestrial and mangrove inputs, shaped by both photodegradation and microbial processing (Huguet et al.,  
 2009). High HIX values ( $> 30$ , Fig. 8) support the presence of well-transformed, highly degraded and older OM, while elevated  
 400 BIX values ( $> 0.6$ ) indicate a marked microbial contribution to DOM transformation, even under extreme constraints.  
 Interestingly, high BIX values may also reflect a contribution from microorganism such as microphytobenthos (MPB), which  
 are known to colonize upper intertidal zones in tropical estuary surrounded by mangrove forest (Haro et al., 2025). Butturini  
 et al. (2022) reported high BIX values ( $\sim 0.7$ ) and significant *in-situ* DOM production in hypersaline shallow lakes ( $> 30\%$   
 salinity) in semi-arid region of Spain. In their study, the microbial-derived DOM was enriched in small, highly oxygenated  
 405 molecules ( $O/C > 0.9$ ), revealing active microbial processing under osmotic stress. In contrast, although salt-flat soils also  
 showed strong microbial signals (mean BIX =  $0.6 \pm 0.03$ ), they did not exhibit similar DOM accumulation. This may suggest  
 that in the present system, photodegradation and mineralization processes, enhanced by intense sunlight and short period of  
 immersion, likely exceed DOM production. This interpretation aligns with Gonsior et al. (2013), who showed that solar  
 irradiation can rapidly degrade DOM in exposed aquatic environments.

410 In the *A. marina* stand, the organic content is higher than in the salt-flat (Fig. 4 and 5), leading to specific  
 biogeochemical characteristics, such as a more acidic pH resulting from OM degradation (Clark et al., 1998). Porewater salinity  
 in this habitat remains relatively high ( $> 50\%$  up to  $80\%$ , Fig. 4), consistent with previous observations in semi-arid  
 mangroves of New Caledonia (Marchand et al., 2011; Deborde et al., 2015). Although *A. marina* is considered salt-tolerant  
 species, its optimal growth is observed under lower salinity levels (300 mM NaCl, approximately  $17.5\%$ ), as shown under  
 415 controlled conditions (Barhoumi et al., 2021). The elevated salinity levels in our study may impose physiological stress,  
 potentially reducing biomass production (Deborde et al., 2015; Leopold et al., 2016). Reduced productivity under these high  
 salinity conditions could limit the OM inputs to the soil and contribute to the lower TOC and DOC values observed in the *A.*  
*marina* stand compared to *R. stylosa* stands (Fig. 5). The DOC concentrations measured under *A. marina* in the present study  
 ( $22 \pm 9$  to  $38 \pm 18$  mg·L<sup>-1</sup>) are within the lower range of values reported for *Avicennia*-dominated mangroves in other tropical  
 420 regions. For example, Yin et al. (2023) reported average DOC concentrations of 49 mg·kg<sup>-1</sup> in a mangrove forest in southeast  
 China dominated by three species, including *Avicennia marina*. Similarly, Marchand et al. (2006) reported average DOC  
 concentrations of  $\sim 30$  to  $90$  mg·L<sup>-1</sup> in *Avicennia*-dominated mangroves in French Guiana. These higher DOC values may  
 result from greater freshwater inputs, as those systems exhibited lower salinity levels ( $< 40\%$ ), which could favour biomass  
 production and/or allochthonous OM input. However, another hypothesis may link to higher nutrient availability in humid  
 425 tropical mangroves, such as nitrogen and phosphorus, that could contribute to increased DOM production (Reef et al., 2010).



This contrasts with our semi-arid study site, which experiences no freshwater input and is bordered by an oligotrophic lagoon, providing limited nutrient inputs.

Beyond quantity, DOM quality in *A. marina* soils also reveals distinctive features, with signatures indicating fresher and less degraded material than in the salt-flat. Canopy cover limits photodegradation, however, DOM appears to be microbially transformed as indicated by elevated BIX values and the predominance of C3% (Wauthy et al., 2018; Hong et al., 2021). In addition, lower HIX values (Fig. 7) and higher SUVA (>5) indicate a greater aromatic content. Microbial activity in *A. marina* soils is likely favoured by pneumatophores, which improve soil aeration and promote aerobic degradation of labile DOM (Kristensen et al., 2008). This dynamic is further supported by recent findings of high bacterial diversity in *A. marina* rhizospheres, underlining the microbial role in DOM transformation (Ghabban et al., 2024). This activity could be linked to the presence of MPB at the soil surface, which have been shown to be abundant in tropical and semi-arid mangroves, even under light-limited conditions beneath dense canopies (Loo et al., 2024). Given the lower canopy density of *A. marina* compared to *R. stylosa* in our study area, light availability is likely higher in *Avicennia* stand, potentially enhancing MPB photosynthetic activity and contributing to the DOM pool (Leopold et al., 2013).

*R. stylosa* stands exhibited the highest OM concentrations of all three stands (TOC, DOC) (Fig. 5). This aligns with other results reported by Dittmar et al. (2006), Kristensen et al. (2008), Arnaud et al. (2023) and Robin et al. (2024a). However, in the present study, DOC concentrations (average around 50 mg·L<sup>-1</sup>) were lower than for tropical mangroves. For instance, Marchand et al. (2006) measured DOC levels up to 300 mg·L<sup>-1</sup> in mature *Rhizophora*-dominated mangroves of French Guiana, and Mori et al. (2019) report DOC concentrations reaching up to 430 μmol·L<sup>-1</sup> in a subtropical estuary in Australia. These higher DOC levels in tropical mangroves likely reflect greater primary productivity and biomass turnover under more favourable hydrological conditions, contrasting with the semi-arid, high-salinity environment of our study site. Another hypothesis for the lower productivity could be nutrient limitation. Mangroves at low latitudes, such as in our semi-arid site, are known to evolve in nutrient-poor conditions, especially low phosphorus availability (Lovelock et al., 2007; Reef et al., 2010). In this context, local hydrological conditions play an additional role. The *R. stylosa* site remains submerged most of the tidal cycle, leading to higher soil moisture and lower evaporation (Baltzer et al., 1982; Marchand et al., 2011). Consequently, salinity remains moderate (~45 ‰), lower than in *A. marina* or salt-flat soils, though still slightly elevated compared to earlier New Caledonian records (~5–40 ‰; Deborde et al., 2015; Marchand et al., 2016).

In this stand, the dominance of the humic-like fluorescent component C2 (Fig. 7) suggests that DOM is primarily mangrove-derived. This is consistent with δ<sup>13</sup>C isotopic analyses on soil samples showing that *R. stylosa* stands contain more mangrove-derived OM than *A. marina* or salt flat habitat (Deborde et al., 2015). In addition, spectroscopic indices (S<sub>275-295</sub>, E<sub>2</sub>/E<sub>3</sub>, SUVA) suggest the accumulation of high-molecular-weight humic substances potentially as a result of the dominance of anoxic conditions (Fig. 4). These results contrast with those of the *A. marina* stands, where microbial processing could be more active and conditions were suboxic due to the specific root system and the shorter length of tidal immersion. The clear decrease in C2% from *R. stylosa* to *A. marina* and its near absence in salt-flats reflects distinct OM sources and transformation pathways across the intertidal landscape.

Interestingly, despite that the DOC concentrations are the highest under *R. stylosa*, FDOM concentrations (measured in QSU, Tab. S6) remain lower than in *A. marina* soils. One possible hypothesis is the adsorption of humic-like DOM onto iron-bearing mineral phases, such as oxides or hydroxides, which are present in *R. stylosa* soils, as supported by XRD data (Fig.8). Iron oxyhydroxide mineral are form in suboxic conditions typical of *Rhizophora* soils (Noël et al., 2014), and can strongly adsorb aromatic FDOM compounds (Lv et al., 2016), especially humic-like components identified by PARAFAC (Groeneweld et al., 2020). Such adsorption processes likely reduce their fluorescence signal in porewater. Additionally, other processes could attenuate FDOM signals such as metal complexation with DOM, that may induce fluorescence quenching (Mounier et al.,



2011). In contrast, *A. marina* stands exhibit a higher contribution of microbially-derived FDOM (C3; Tab. S6), which is most resistant to adsorption onto minerals and may remain more bioavailable in the dissolved phase (Groeneveld et al., 2020).

470 Additionally, this stand was characterized by lower pH values. This could partly be the result of greater accumulation of organic acid from root exudates (Arnaud et al., 2023) and leaf litter decomposition (Hinsinger et al., 2003; Robin et al., 2024a; Robin et al., 2024b). However, acidic pH values can also reflect the oxidation of pyrite, which is commonly observed in suboxic mangrove soils (Kristensen et al., 2017). This interpretation is supported by our XRD data (Fig. 8), which reveal the presence of pyrite (FeS<sub>2</sub>) and iron sulfates such as jarosite, which is indicative of sulfur oxidation processes under suboxic and oxic conditions. This oxidation process leads to the release of H<sup>+</sup> ions, further contributing to soil acidification and potentially  
 475 influencing DOM cycling. This process also led to the production of dissolved iron and its precipitation as oxides or hydroxides (Noël et al., 2014). These findings suggest that the physicochemical interactions between DOM and soil minerals, particularly under *R. stylosa* stands, may significantly modulate the composition and fluorescence of DOM in mangrove soils.

This spatial pattern between the 3 intertidal zones supported by PCA results (Fig. 2), reveal a clear separation of DOM composition along the intertidal gradient. The first principal component (PC1) captures the contrast between land-derived OM  
 480 (C1), dominant in the salt-flat, and mangrove-derived OM (C2), which increases seaward. This spatial pattern suggests that tidal movements influence DOM dynamics within the mangrove system itself, by facilitating the input of terrestrial compounds from upper zones toward lower, while mangrove-derived humic substances may accumulate in more frequently flooded zones. The photo-degradation marker C4, observed in similar proportions across habitats, indicates that UV exposure affects DOM composition uniformly, making it a poor tracer for spatial differentiation. Taken together, these patterns suggest that: i) C1  
 485 likely reflects photodegraded humic substances; ii) C2 is associated with mangrove-derived OM; iii) C3 indicates microbial activity; and iv) C4 corresponds to photo-degradation but lacks spatial variability. These results highlight the importance of habitat zonation related to climatic conditions, particularly aridity and tidal influence, in structuring DOM composition and distribution in semi-arid mangroves ecosystems, and reinforce the key role of *R. stylosa* stands in OM accumulation and transformation (Dittmar et al., 2006; Kristensen et al., 2008).

490 While intertidal zonation related to the semi-arid climate and hydrodynamics clearly control spatial variability in DOM, our results also suggest that seasonal changes in environmental conditions, particularly between the dry and wet seasons, can further modulate DOM inputs, composition, and microbial processing. The following section explores how this seasonal variability interacts with habitat-specific processes to influence DOM dynamics across the land-sea gradient.

#### 4.2 Seasonal variability of DOM quality and quantity in mangrove soils

495 In mangrove soils, DOM originates from both vascular plant material (leaf litter, root exudates) (Arnaud et al., 2023; Robin et al., 2024a) and primary producers such as microphytobenthos (MPB) (Loo et al., 2024). These sources contribute to DOM through leaching and microbial decomposition, which can vary between seasons. As a result, DOM quantity and composition are expected to vary not only across habitats, as discussed in the previous section, but also between seasons, depending on source activity and transformation pathways.

500 In the present study, environmental conditions, including temperature, precipitation, and evaporation, varied significantly between the two seasons (Fig.3). The rainy and warm season recorded 32% more precipitation than the dry season, although a rainfall event was observed one month before the dry season sampling. These seasonal differences had a significant impact on the physico-chemical properties of the soil, particularly salinity, redox potential (Eh), and pH, influencing biogeochemical processes across the three studied habitats as described in the previous section. Salinity was always higher during the dry  
 505 season in all three zones, with the most pronounced difference observed at the upstream site along the intertidal gradient. This increase in salinity can be attributed to high evaporation rates in the salt-flat, where porewater salinity reached up to 120 ‰





during the dry season compared to 90 % in the wet season. Redox potential (Eh) values decreased from the salt-flat to the *R. stylosa* site during the wet season. However, the contrast between *A. marina* and *R. stylosa* was less pronounced during the dry season, suggesting seasonal modulation of redox conditions. In contrast, no significant seasonal difference in redox potential was observed under the *R. stylosa* stand, likely due to more frequent inundation at these sites due to their lower position along the intertidal gradient (Marchand et al., 2011). Regarding pH, soil acidity increased during the rainy and warm season across all habitats. While this difference was not significant for the salt-flat, it was significant in the *A. marina* and *R. stylosa* stands. This seasonal acidification may be driven by the introduction of electron acceptors via rainwater infiltration, stimulating microbial respiration and sulfur oxidation, both of which contribute to H<sup>+</sup> release. Another hypothesis is that higher temperatures during the wet season may stimulate biological activity, accelerating the decomposition of OM and leading to increased production of organic acids, which in turn lowers pH (Leopold et al., 2015; Vinh et al., 2019).

TOC concentrations increased during the wet and warm season in both salt-flat and *A. marina* soils, likely reflecting enhanced OM input or production during this period. Higher DOC concentrations during the wet and warm season, as observed in previous studies (Kathiresan et al., 2013; Sanyal et al., 2020), suggest increased DOM production due to enhanced leaf leaching during the rainy period. In contrast, TOC and DOC concentrations in *R. stylosa* soils remained stable across seasons, but consistently higher than in the two other habitats (Fig.4). These stable concentrations may be attributed to the continuous supply of OM, such as root exudates and mangrove-derived particulate material, supported by their low position along the intertidal gradient, where tidal immersion occurs daily regardless of season allowing a constant leaching.

Beyond DOM quantity, seasonal variations also influenced DOM quality and degree of transformation. These variations were particularly marked in the salt-flat, where OM content was lowest. The increase in E<sub>2</sub>/E<sub>3</sub> during the dry season may reflect enhanced DOM photodegradation (Huguet et al., 2009) or from MPB activity (Haro et al., 2025), whereas lower values in the wet season indicate a greater contribution of less degraded OM. A similar seasonal trend was observed with S<sub>275-295</sub>, further supporting the dominance of degraded OM in the dry season. These indices highlight how seasonality modulates DOM transformation pathways, particularly in vegetation-poor systems like the salt-flat. In contrast, SUVA, (a proxy for aromaticity and humification) revealed different seasonal trends between the vegetated sites. *A. marina* soils SUVA values significantly decreased during the wet and warm season (from ~10 to ~5; p < 0.05), suggesting a fresher, more labile DOM. This likely reflects increased inputs of autochthonous material, including microbial and algal production, potentially stimulated by nutrient inputs from rainfall and reduced salinity stress (Chowdhury et al., 2019; Ghabban et al., 2024; Robin et al., 2024b). The increase in DOM quantity (DOC, CDOM) and the rise in the biologically-derived component C<sub>3</sub> during the wet season further support this hypothesis (Fig. 5). Together, these patterns suggest that both leaching of plant-derived compounds and enhanced biological productivity contribute to the seasonal enrichment in fresher and more bioavailable DOM.

Among the potential DOM sources, MPB likely play a significant role, especially during the wet and warm season. These benthic microalgae are known to develop in intertidal mangrove sediments, even under canopy cover (Loo et al., 2024). Their abundance varies with mangrove zonation, as previously discussed, but also shows strong seasonal dynamics. Several studies have demonstrated that MPB biomass and productivity increase during the warm and wet season (Leopold et al., 2013; Molnar et al., 2014; Jacotot et al., 2018), particularly following initial rainfall events that stimulate microbial activity and labile DOM release (Vinh et al., 2019). In our study, this seasonal dynamic is particularly evident in *A. marina* stands, where canopy density is lower and light penetration greater than in *R. stylosa*. Enhanced biological activity in this habitat during the wet season is supported by increased C<sub>3</sub> fluorescence, typically associated with autochthonous microbial production, along with higher BIX values and lower SUVA indices, indicating a DOM pool that is fresher, less aromatic, and microbially derived. Similarly, BIX values in both vegetated habitats (*A. marina* and *R. stylosa*) were significantly higher in the wet season (Fig. 7). This suggests that microbial processes are more active during the wet and warm season, a hypothesis supported by studies



showing that carbon metabolic activity is three times higher during the rainy season compared to the dry season (Wang et al., 2024). Furthermore, the HIX (Fig. 7) confirms that OM in *A. marina* soils was less humified and degraded in the wet season, consistent with the influx of fresher material. Consequently, we suggest that lower salinity and increased water availability in the wet season likely stimulate *A. marina* growth and DOM production, while in the dry season, physiological stress from elevated salinity may lead to reduced productivity and increased exudation of more refractory compounds (Garcia et al., 2017). Regarding lateral carbon transport, the gradient of C2% fluorescence among the three sites was more pronounced during the dry season, suggesting that C2 is transported by tidal action from *R. stylosa* to salt-flat, while C1 is exported from salt-flat to the *A. marina* and *R. stylosa* stands. However, the increased presence of C1, typically associated with degraded DOM, could also result from in situ degradation of DOM originally produced by microorganisms. This additional pathway would suggest that local transformation processes, mixing with tidal movement, contribute to shaping DOM composition across habitats. This supports the hypothesis that tide-driven lateral export may play a key role in carbon distribution within mangroves (Donato et al., 2011; Ohtsuka et al., 2020). Eventually, the C4 component, associated with photo-degradation, previously documented in multiple studies (Amaral et al., 2020; Lambert et al., 2016; Chen et al., 2017; Hong et al., 2021) (Tab. A5), was more abundant in the wet season. This may appear counterintuitive but could be due to the increased availability of fresh DOM, making it more vulnerable to photodegradation, with light exposure and temperature (Amaral et al., 2020; Lambert et al., 2016).

These findings highlight the complexity of OM dynamics in mangrove ecosystems, raising important questions about the origins, degradation pathways, and export processes of DOM.

## 5 Conclusion and perspectives

By examining DOC, CDOM, and FDOM across the three intertidal habitats studied (salt-flat, *Avicennia marina*, and *Rhizophora stylosa*), this study provides new insights into carbon cycling in mangrove ecosystems developing in semi-arid climate. We measured significant spatial (land-sea gradient) and seasonal (wet and dry season) variations in DOM quality and quantity. *R. stylosa* stands, located at the seaward fringe, had the highest and most stable DOM concentrations throughout the year, likely due to regular OM inputs from litterfall and root exudates, combine with regular tidal immersion inducing constant leaching. In contrast, the salt-flat exhibited the lowest DOM concentrations and the greatest seasonal fluctuations, highlighting their sensitivity to allochthonous inputs and exposure to sunlight. *A. marina* stands presented intermediate characteristics, with fresher and more labile OM, specifically during the wet season.

Seasonal variability had a different influence depending on habitat. In the salt-flat, the absence of vegetation led to pronounced changes in DOM concentration and quality. In *A. marina*, lower salinity during the wet season may stimulate productivity and microbial transformation of the DOM, as evidenced by a reduction in SUVA and an increase in BIX. Concerning the *R. stylosa* stand, characterized by continuous tidal submersion, only a few seasonal changes were observed. However, tidal fluctuations in this stand are a major cause for continuous Fe reduction-oxidation cycles, and adsorption of humic-like DOM onto iron-bearing mineral phases is suspected, which may explain lower FDOM concentrations than in *A. marina* soils.

The spatial distribution of FDOM components revealed distinct trends: C1 (terrestrial or highly degraded) declined from land to sea, while C2 (mangrove-derived) decreased landward, suggesting bidirectional OM distribution along the intertidal gradient. These patterns point to tidal-driven lateral transport as a key mechanism driving DOM dynamics, regulated by vegetation structure and soil properties. However, the relative importance of lateral transport compared to local production and degradation remains to be fully quantified. Future studies should aim to quantify these fluxes and explore molecular markers (e.g., lignin phenols) to trace OM sources more precisely. Understanding how hydrology, vegetation, and seasonality interact



to regulate OM export is essential for improving carbon budget assessments and conservation strategies for these blue carbon ecosystems.

## 6 Appendix A

590 **Table A1: PERMANOVA analysis of Bouraké sediment and porewater composition, based on fourth-root transformed data and bray-curtis dissimilarities**

Factor	df	SumOfSqs	R <sup>2</sup> (%)	F-value	p-value
Season	1	0.3093	4.8%	7.75	0.004
Habitat	2	4.0760	63.1%	51.06	0.001
Depth	2	0.1604	2.4%	2.01	0.1
Residuals	48	1.9159	29.7%		
Total	53	6.4616	100%		



595 **Table A2: Mean concentrations ( $\pm$  SD) of clay, silt, sand, and total organic carbon (TOC, in %) in soils across the three mangrove habitats (salt-flat: Sa, *Avicennia marina*: Av, *Rhizophora stylosa*: Rh), at three depth intervals (0-10 cm, 10-20 cm, 20-30 cm), for both dry and wet seasons. Bold values indicate the mean values, while standard deviations are presented in regular font.**

Site	Depth (cm)	Clay (%)		Silt (%)		Sand (%)		TOC (%)	
		WET	DRY	WET	DRY	WET	DRY	WET	DRY
Sa	0-10	<b>7.3</b> $\pm$ 4.1	<b>8.5</b> $\pm$ 7.3	<b>85.2</b> $\pm$ 7.0	<b>47.1</b> $\pm$ 25	<b>7.5</b> $\pm$ 8.7	<b>44.4</b> $\pm$ 32.8	<b>0.6</b> $\pm$ 0.2	<b>2.0</b> $\pm$ 0.1
	10-20	<b>16.0</b> $\pm$ 7.2	<b>9.6</b> $\pm$ 4.8	<b>78.9</b> $\pm$ 3.7	<b>49.3</b> $\pm$ 20	<b>5.1</b> $\pm$ 5.6	<b>41.1</b> $\pm$ 25.1	<b>0.6</b> $\pm$ 0.1	<b>2.0</b> $\pm$ 0.2
	20-30	<b>24.8</b> $\pm$ 7.5	<b>7.6</b> $\pm$ 7.9	<b>73.3</b> $\pm$ 6.1	<b>41.0</b> $\pm$ 28	<b>1.9</b> $\pm$ 3.1	<b>51.3</b> $\pm$ 36.4	<b>0.7</b> $\pm$ 0.3	<b>1.9</b> $\pm$ 0.0
Av	0-10	<b>12.8</b> $\pm$ 6.8	<b>11.7</b> $\pm$ 1.2	<b>77.1</b> $\pm$ 6.7	<b>71.7</b> $\pm$ 12.7	<b>10.1</b> $\pm$ 8.9	<b>16.5</b> $\pm$ 13.0	<b>2.2</b> $\pm$ 0.1	<b>4.0</b> $\pm$ 0.4
	10-20	<b>16.4</b> $\pm$ 4.7	<b>13.6</b> $\pm$ 1.0	<b>82.8</b> $\pm$ 4.2	<b>72.4</b> $\pm$ 5.5	<b>0.7</b> $\pm$ 1.1	<b>14.0</b> $\pm$ 5.0	<b>1.2</b> $\pm$ 0.3	<b>2.8</b> $\pm$ 0.2
	20-30	<b>13.2</b> $\pm$ 4.5	<b>12.8</b> $\pm$ 2.5	<b>72.8</b> $\pm$ 8.1	<b>75.3</b> $\pm$ 8.8	<b>14.0</b> $\pm$ 12.1	<b>11.9</b> $\pm$ 9.5	<b>1.8</b> $\pm$ 1.0	<b>4.5</b> $\pm$ 2.3
Rh	0-10	<b>13.2</b> $\pm$ 5.1	<b>6.1</b> $\pm$ 1.0	<b>84.4</b> $\pm$ 3.4	<b>86.7</b> $\pm$ 1.2	<b>2.3</b> $\pm$ 1.6	<b>7.1</b> $\pm$ 2.1	<b>10.4</b> $\pm$ 1.3	<b>10.1</b> $\pm$ 1.0
	10-20	<b>12.9</b> $\pm$ 3.5	<b>6.3</b> $\pm$ 1.2	<b>85.1</b> $\pm$ 2.4	<b>80.2</b> $\pm$ 9.5	<b>1.9</b> $\pm$ 1.4	<b>13.5</b> $\pm$ 10.5	<b>9.7</b> $\pm$ 0.7	<b>9.4</b> $\pm$ 0.4
	20-30	<b>10.8</b> $\pm$ 0.6	<b>6.4</b> $\pm$ 0.1	<b>86.9</b> $\pm$ 2.2	<b>85.3</b> $\pm$ 6.1	<b>2.3</b> $\pm$ 1.6	<b>8.3</b> $\pm$ 6.1	<b>8.3</b> $\pm$ 1.2	<b>8.7</b> $\pm$ 0.5



600 **Table A3: Mean Values ( $\pm$ SD) of Salinity, pH, and Redox Potential (Eh in mV), Density (g/m<sup>3</sup>), water content (%) and Temperature (c°) across three mangrove habitats (salt-flat: Sa, *Avicennia marina*: Av, *Rhizophora stylosa*: Rh) at three depth intervals (0-10 cm, 10-20 cm, 20-30 cm) along sedimentary cores for Dry and Wet seasons. Bold values indicate the mean values, while standard deviations are presented in regular font.**

Site	Depth (cm)	Salinity		pH		Eh (mV)		Density (g/cm <sup>3</sup> )		Water content (%)		Temperature (C°)	
		WET	DRY	WET	DRY	WET	DRY	WET	DRY	WET	DRY	WET	DRY
Sa	0-10	<b>106</b> $\pm$ 8.54	<b>153</b> $\pm$ 3.0	<b>7.48</b> $\pm$ 0.14	<b>7.62</b> $\pm$ 0.09	<b>367</b> $\pm$ 99.15	<b>409</b> $\pm$ 53.3	<b>1.4</b> $\pm$ 0.1	<b>1.4</b> $\pm$ 0.0	<b>22.1</b> $\pm$ 2.9	<b>20.6</b> $\pm$ 1.7	<b>25.7</b> $\pm$ 0.7	<b>29.4</b> $\pm$ 0.7
	10-20	<b>84</b> $\pm$ 5.13	<b>104</b> $\pm$ 14.2	<b>6.98</b> $\pm$ 0.19	<b>7.23</b> $\pm$ 0.24	<b>121</b> $\pm$ 22.8	<b>427</b> $\pm$ 30.9	<b>1.5</b> $\pm$ 0.1	<b>1.4</b> $\pm$ 0.1	<b>25.3</b> $\pm$ 1.2	<b>26.6</b> $\pm$ 4.0	<b>24.5</b> $\pm$ 0.5	<b>28.4</b> $\pm$ 0.0
	20-30	<b>74</b> $\pm$ 7.94	<b>95</b> $\pm$ 10	<b>6.60</b> $\pm$ 0.22	<b>6.82</b> $\pm$ 0.08	<b>116</b> $\pm$ 34.9	<b>482</b> $\pm$ 32.8	<b>1.4</b> $\pm$ 0.1	<b>1.3</b> $\pm$ 0.1	<b>28.8</b> $\pm$ 2.5	<b>30.3</b> $\pm$ 3.8	<b>23.8</b> $\pm$ 0.5	<b>28.1</b> $\pm$ 0.0
Av	0-10	<b>56</b> $\pm$ 3.46	<b>56</b> $\pm$ 3.0	<b>6.49</b> $\pm$ 0.04	<b>6.72</b> $\pm$ 0.26	<b>85</b> $\pm$ 23	<b>-101</b> $\pm$ 76.5	<b>1.1</b> $\pm$ 0.1	<b>0.9</b> $\pm$ 0.0	<b>37.8</b> $\pm$ 5.7	<b>48.0</b> $\pm$ 3.5	<b>23.5</b> $\pm$ 0.3	<b>26.7</b> $\pm$ 0.4
	10-20	<b>57</b> $\pm$ 2.64	<b>56</b> $\pm$ 2.3	<b>6.57</b> $\pm$ 0.05	<b>6.87</b> $\pm$ 0.1	<b>59</b> $\pm$ 20	<b>-114</b> $\pm$ 12.1	<b>1.3</b> $\pm$ 0.1	<b>0.9</b> $\pm$ 0.1	<b>30.8</b> $\pm$ 3.6	<b>40.9</b> $\pm$ 2.2	<b>22.3</b> $\pm$ 0.2	<b>27.9</b> $\pm$ 0.4
	20-30	<b>57</b> $\pm$ 2.51	<b>53</b> $\pm$ 3.5	<b>6.62</b> $\pm$ 0.02	<b>6.93</b> $\pm$ 0.06	<b>55</b> $\pm$ 6.8	<b>-91</b> $\pm$ 33.1	<b>1.2</b> $\pm$ 0.2	<b>0.8</b> $\pm$ 0.2	<b>34.3</b> $\pm$ 6.1	<b>46.7</b> $\pm$ 9.3	<b>21.8</b> $\pm$ 0.2	<b>27.6</b> $\pm$ 1.3
Rh	0-10	<b>45</b> $\pm$ 1.73	<b>46</b> $\pm$ 3.0	<b>5.97</b> $\pm$ 0.11	<b>6.00</b> $\pm$ 0.12	<b>29</b> $\pm$ 106	<b>-105</b> $\pm$ 30.6	<b>0.5</b> $\pm$ 0.0	<b>0.5</b> $\pm$ 0.0	<b>60.1</b> $\pm$ 2.3	<b>61.7</b> $\pm$ 1.2	<b>22.1</b> $\pm$ 0.6	<b>27.6</b> $\pm$ 0.8
	10-20	<b>46</b> $\pm$ 2.08	<b>47</b> $\pm$ 2.6	<b>6.04</b> $\pm$ 0.12	<b>6.3</b> $\pm$ 0.01	<b>-114</b> $\pm$ 15.1	<b>-176</b> $\pm$ 17.0	<b>0.5</b> $\pm$ 0.0	<b>0.5</b> $\pm$ 0.0	<b>60.3</b> $\pm$ 2.6	<b>63.1</b> $\pm$ 1.1	<b>21.6</b> $\pm$ 0.6	<b>26.2</b> $\pm$ 0.1
	20-30	<b>44</b> $\pm$ 1.73	<b>47</b> $\pm$ 1.1	<b>6.05</b> $\pm$ 0.08	<b>6.26</b> $\pm$ 0.08	<b>-129</b> $\pm$ 5.41	<b>-163</b> $\pm$ 23.0	<b>0.5</b> $\pm$ 0.0	<b>0.5</b> $\pm$ 0.0	<b>61.8</b> $\pm$ 3.0	<b>63.7</b> $\pm$ 0.8	<b>21.3</b> $\pm$ 0.3	<b>26.0</b> $\pm$ 0.3



605 Table A4: Mean values ( $\pm$  SD) of Dissolved Organic Carbon (DOC, in  $\text{mg L}^{-1}$ ) and Coloured Dissolved Organic Matter (CDOM, as  $a_{350}$  in  $\text{m}^{-1}$ ,  $S_{275-295}$  in  $\mu\text{m}^{-1}$ , E2/E3, SUVA) across the three mangrove habitats (salt-flat: Sa, *Avicennia marina*: Av, *Rhizophora stylosa*: Rh) for both dry and wet seasons. Bold values indicate the mean values, while standard deviations are presented in regular font.

Site	Depth (cm)	CDOM $a_{350}$ ( $\text{m}^{-1}$ )		$S_{275-295}$ ( $\mu\text{m}^{-1}$ )		DOC ( $\text{mg L}^{-1}$ )		$E_2/E_3$		SUVA	
		WET	DRY	WET	DRY	WET	DRY	WET	DRY	WET	DRY
Sa	0-10	17.50 $\pm$ 3.39	0.08 $\pm$ 0.02	17.2 $\pm$ 0.4	19.0 $\pm$ 0.5	16.81 $\pm$ 1.74	12.53 $\pm$ 2.76	6.62 $\pm$ 0.15	7.67 $\pm$ 0.31	5.03 $\pm$ 1.26	0.03 $\pm$ 0.00
	10-20	12.82 $\pm$ 2.46	0.04 $\pm$ 0.00	18.1 $\pm$ 0.5	23.2 $\pm$ 3.7	17.31 $\pm$ 3.81	12.09 $\pm$ 1.44	7.00 $\pm$ 0.19	8.58 $\pm$ 0.80	3.73 $\pm$ 1.03	0.02 $\pm$ 0.00
	20-30	13.66 $\pm$ 3.92	0.04 $\pm$ 0.01	19.4 $\pm$ 0.6	24.0 $\pm$ 3.9	17.00 $\pm$ 1.27	11.89 $\pm$ 2.89	5.96 $\pm$ 1.37	8.96 $\pm$ 1.52	3.90 $\pm$ 0.83	0.02 $\pm$ 0.00
Av	0-10	140.87 $\pm$ 29.41	86.52 $\pm$ 9.94	6.6 $\pm$ 1.6	8.1 $\pm$ 3.2	30.14 $\pm$ 1.19	25.32 $\pm$ 16.90	1.60 $\pm$ 0.21	1.81 $\pm$ 0.48	6.99 $\pm$ 0.70	7.62 $\pm$ 4.23
	10-20	50.82 $\pm$ 35.61	91.20 $\pm$ 52.94	16.3 $\pm$ 4.0	12.0 $\pm$ 6.9	55.31 $\pm$ 26.87	18.82 $\pm$ 2.59	4.89 $\pm$ 1.88	3.08 $\pm$ 2.21	3.24 $\pm$ 1.17	9.86 $\pm$ 2.18
	20-30	44.14 $\pm$ 10.36	48.52 $\pm$ 11.18	16.4 $\pm$ 2.7	19.5 $\pm$ 0.3	29.44 $\pm$ 6.83	23.57 $\pm$ 2.52	4.61 $\pm$ 1.37	5.48 $\pm$ 0.13	5.29 $\pm$ 1.05	8.46 $\pm$ 1.10
Rh	0-10	47.90 $\pm$ 28.66	51.66 $\pm$ 20.48	8.8 $\pm$ 7.6	15.1 $\pm$ 4.4	35.34 $\pm$ 45.14	52.65 $\pm$ 51.56	2.82 $\pm$ 2.46	4.08 $\pm$ 1.20	6.29 $\pm$ 4.92	4.88 $\pm$ 2.96
	10-20	43.30 $\pm$ 24.35	43.45 $\pm$ 10.58	16.0 $\pm$ 0.6	18.1 $\pm$ 0.7	49.44 $\pm$ 33.32	42.55 $\pm$ 13.21	4.68 $\pm$ 0.72	4.96 $\pm$ 0.08	3.38 $\pm$ 0.62	4.00 $\pm$ 1.04
	20-30	56.50 $\pm$ 28.55	64.25 $\pm$ 54.14	15.2 $\pm$ 4.5	16.7 $\pm$ 2.3	50.75 $\pm$ 30.83	65.33 $\pm$ 28.66	4.49 $\pm$ 0.82	5.03 $\pm$ 0.41	4.44 $\pm$ 1.98	3.53 $\pm$ 1.85



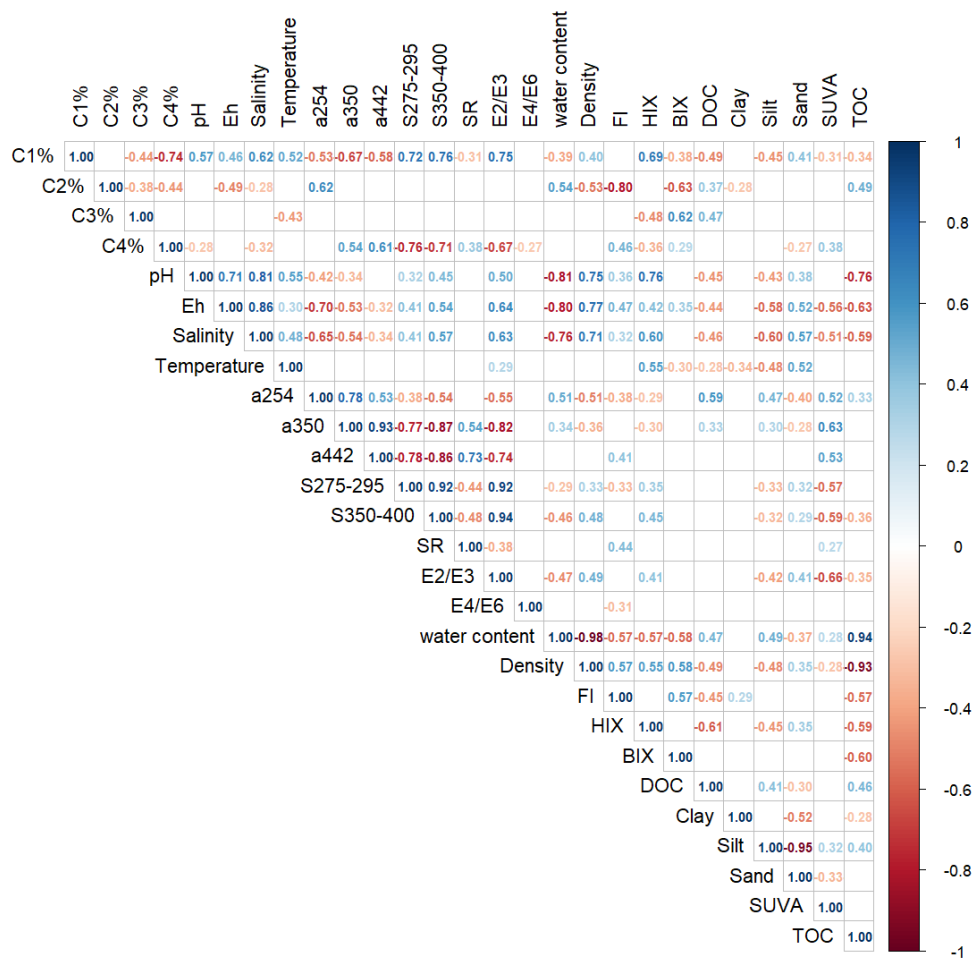
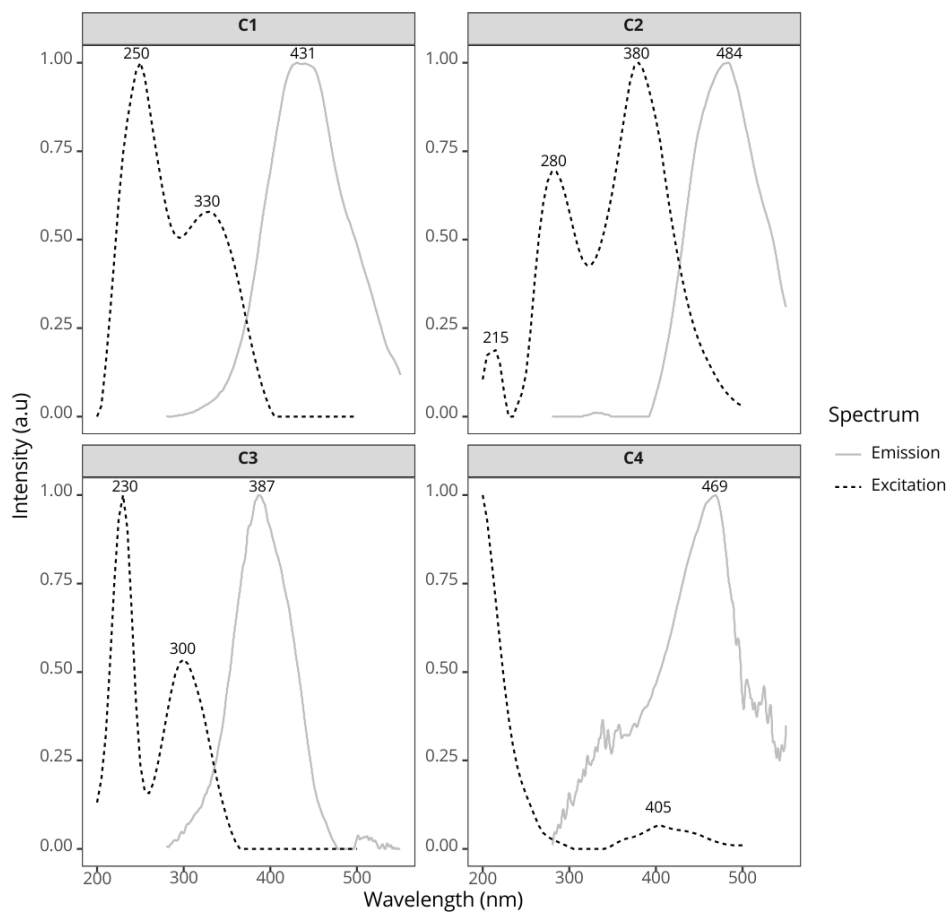
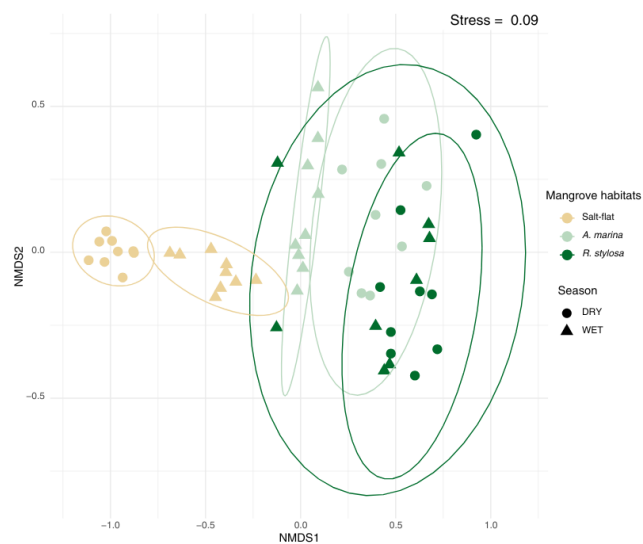


Figure A1: Spearman correlation matrix showing relationships among granulometric properties, carbon content (TOC, DOC), optical DOM indices (CDOM, FDOM), and physicochemical parameters (pH, salinity, temperature, redox potential, water content, and density).



615 **Figure A2: Excitation and emission spectra of the four fluorescent components identified using the PARAFAC model, showing their respective excitation and emission maxima.**



620

**Figure A3:** Non metric multidimensional scaling (nMDS) ordination of sampling units based on Bray-Curtis dissimilarities of standardized environmental variables in a total of  $N = 54$  sampling units ( $n = 3$  replicates from each of the three mangrove habitat at 3 depths during 2 seasons) in the Bouraké mangrove ecosystem. Colours indicate the mangroves habitat; ellipse represent clusters and symbols show seasons.

625



**Table A5: Identification of fluorophores and comparison of the spectral characteristic of the components identified in Bouraké (June - October 2023) with those of other study uploaded on Open Fluor database with a spectral match of Tucker's correlation coefficient > 0.95**

Component Bouraké season 2023			Other study						
$\lambda_{ex}$ (nm)	$\lambda_{em}$ (nm)	Type	Comp.	$\lambda_{ex}$ (nm)	$\lambda_{em}$ (nm)	Reference	Type	Origin	Environment
C1 250(330)	431	Terrestrial Humic-like	C1	320(250)	428	(Walker et al., 2009)	humic	terrestrially derived material	Seawater arctic
			C1	333	440	(Smith et al., 2021)	humic acids	Humic-like fluorophore of terrestrial origin; derived from processing of DOM by terrestrial or aquatic microbes in forested streams,	Urban coastal ecosystem
			C1	245(320)	442	(Yang et al., 2024)	Humic-like	Plant and soil derived ; lignin-phenols as FDOM source	River water
C2 215(280)380	484	Terrestrial Humic like	C2	390	475	(Maurischat et al., 2022)	Terrestrial-like	Identify in various lakes, estuaries, and coastal waters	Lake
			C1	275(375)	477	(Liu et al., 2019)	Terrestrially-derived humic material		Lake sediments
			Comp2	365	510	(Hong et al., 2021)	Natural soil fulvic ; humic-like		saltmarsh
			C3	395(270)	450	(Jeonghyun et al., 2020)	terrestrial humic-like peak		seawater and river
C3 230(300)	387	Marine-humic-like	Comp4	310	380(530)	(Hong et al., 2021)	Marine humic-like	Marine Humic-like ; microbially derived allochthonous	saltmarsh
			C2	<250 (303)	380	(Smith et al., 2021)	Marine humic-like	Marine environments with biological activity	Urban coastal ecosystem
			Comp4	300	386	(Wauthy et al., 2018)	Humic-like	microbial origin	Seawater
C4 <200	469	Humic-like Photo-product	Comp3	<250	455	(Hong et al., 2021)	Humic-like Photo-product	terrestrial humic-like ; photo-product	saltmarsh
			C4	250	430	(Amaral et al., 2020)	Humic-like Photo-product	terrestrially derived component ; produced after DOM exposure to UV radiation	Coastal
			C2	<260	434	(Chen et al., 2017)	Humic-like Photo-product	terrestrial humic-like ; photo product and/or photo-refractory	Sediment
			C4	<260	444	(Lambert et al., 2016)	Humic-like Photo-product	Terrestrial and photochemically degraded	tropical rivers
			Comp3	<260	448	(Wauthy et al., 2018)	Humic-like		Seawater



**Table A6: Mean values ( $\pm$  SD) of fluorescent components (C1-C4, in quinine sulphate units, QSU) across the three mangrove habitats (salt-flat, *Avicennia marina*, *Rhizophora stylosa*) for both dry and wet seasons**

Habitat	Seasons	C1 (Q.S.U)	C2 (Q.S.U)	C3 (Q.S.U)	C4 (Q.S.U)
salt-flat	DRY	7.70 $\pm$ 1.54	1.80 $\pm$ 0.72	1.65 $\pm$ 0.56	0.58 $\pm$ 0.56
	WET	11.07 $\pm$ 2.29	2.59 $\pm$ 0.70	2.82 $\pm$ 0.87	2.48 $\pm$ 1.09
<i>A. marina</i>	DRY	10.95 $\pm$ 4.12	4.82 $\pm$ 2.60	2.44 $\pm$ 0.82	4.17 $\pm$ 5.79
	WET	11.67 $\pm$ 3.46	4.81 $\pm$ 1.65	12.67 $\pm$ 6.19	9.28 $\pm$ 5.54
<i>R. stylosa</i>	DRY	4.36 $\pm$ 1.48	2.77 $\pm$ 1.21	1.28 $\pm$ 1.27	1.36 $\pm$ 1.29
	WET	4.13 $\pm$ 1.47	2.42 $\pm$ 1.10	2.11 $\pm$ 1.11	2.52 $\pm$ 2.23



635 **Table A7: Results of statistical tests for seasonal differences (between wet and dry season) for each measured parameter within the three habitats. Parametric data were analysed using Student's t-test, while Mann-Whitney U tests were applied for non-parametric distributions. Significance levels are indicated as follows:  $p < 0.05$  (\*),  $p < 0.01$  (\*\*), and  $p < 0.001$  (\*\*\*); N.S = not significant.**

Habitat	Parameter	P-value	Significance	Parametric test	Test used
salt-flat	pH	0.3059	N.S	Yes	t-test
	Eh	0.0104	*	No	Mann-Whitney U
	Salinity	0.0156	*	Yes	t-test
	Temperature	0.0000	***	Yes	t-test
	a <sub>254</sub>	0.0000	***	Yes	t-test
	a <sub>350</sub>	0.0000	***	Yes	t-test
	a <sub>442</sub>	0.0000	***	Yes	t-test
	S <sub>275-295</sub>	0.0064	**	Yes	t-test
	S <sub>350-400</sub>	0.0268	*	Yes	t-test
	SR	0.0392	*	Yes	t-test
	E <sub>2</sub> E <sub>3</sub>	0.0004	***	No	Mann-Whitney U
	E <sub>4</sub> E <sub>6</sub>	0.0861	N.S	Yes	t-test
	Water content	0.8288	N.S	Yes	t-test
	Density	0.5053	N.S	Yes	t-test
	FI	0.8715	N.S	Yes	t-test
	HIX	0.7101	N.S	Yes	t-test
	BIX	0.4454	N.S	Yes	t-test
	DOC	0.0002	***	Yes	t-test
	Clay	0.0625	N.S	Yes	t-test
	Silt	0.0016	**	Yes	t-test
	Sand	0.0020	**	No	Mann-Whitney U
	SUVA	0.0000	***	Yes	t-test
	TOC	0.0000	***	Yes	t-test
	C1%	0.0008	***	Yes	t-test
	C2%	0.3739	N.S	Yes	t-test
	C3%	0.7949	N.S	Yes	t-test
	C4%	0.0018	**	Yes	t-test
<i>A. marina</i>	pH	0.0004	***	Yes	t-test
	Eh	0.0000	***	Yes	t-test
	Salinity	0.4739	N.S	No	Mann-Whitney U
	Temperature	0.0000	***	Yes	t-test
	a <sub>254</sub>	0.9032	N.S	Yes	t-test
	a <sub>350</sub>	0.8801	N.S	Yes	t-test
	a <sub>442</sub>	0.6588	N.S	No	Mann-Whitney U
	S <sub>275-295</sub>	0.6588	N.S	No	Mann-Whitney U
	S <sub>350-400</sub>	0.5365	N.S	No	Mann-Whitney U
	SR	0.3314	N.S	No	Mann-Whitney U
	E <sub>2</sub> E <sub>3</sub>	0.4799	N.S	No	Mann-Whitney U
	E <sub>4</sub> E <sub>6</sub>	0.7775	N.S	Yes	t-test
	Water content	0.0011	**	Yes	t-test
	Density	0.0011	**	Yes	t-test
	FI	0.2893	N.S	No	Mann-Whitney U
	HIX	0.0007	***	Yes	t-test
	BIX	0.0008	***	No	Mann-Whitney U
	DOC	0.0062	**	No	Mann-Whitney U
	Clay	0.4452	N.S	Yes	t-test
	Silt	0.2448	N.S	Yes	t-test
	Sand	0.1118	N.S	No	Mann-Whitney U
	SUVA	0.0051	**	Yes	t-test
	TOC	0.0013	**	Yes	t-test
	C1%	0.0030	**	Yes	t-test
	C2%	0.0176	*	Yes	t-test
	C3%	0.0009	***	Yes	t-test
	C4%	0.4832	N.S	Yes	t-test
<i>R. stylosa</i>	pH	0.0187	*	Yes	t-test
	Eh	0.0518	N.S	No	Mann-Whitney U
	Salinity	0.0382	*	Yes	t-test





	Temperature	0.0004	***	No	Mann-Whitney U
	a <sub>254</sub>	0.2164	N.S	No	Mann-Whitney U
	a <sub>350</sub>	0.7239	N.S	No	Mann-Whitney U
	a <sub>442</sub>	0.7237	N.S	No	Mann-Whitney U
	S <sub>275-295</sub>	0.1333	N.S	No	Mann-Whitney U
	S <sub>350-400</sub>	0.1740	N.S	Yes	t-test
	SR	0.9296	N.S	No	Mann-Whitney U
	E <sub>2</sub> E <sub>3</sub>	0.4799	N.S	No	Mann-Whitney U
	E <sub>4</sub> E <sub>6</sub>	0.2877	N.S	Yes	t-test
	Water content	0.0382	*	Yes	t-test
	Density	0.0990	N.S	Yes	t-test
	FI	0.2510	N.S	No	Mann-Whitney U
	HIX	0.2164	N.S	No	Mann-Whitney U
	BLX	0.0134	*	No	Mann-Whitney U
	DOC	0.5921	N.S	Yes	t-test
	Clay	0.0005	***	Yes	t-test
	Silt	0.9296	N.S	No	Mann-Whitney U
	Sand	0.0006	***	No	Mann-Whitney U
	SUVA	0.6364	N.S	Yes	t-test
	TOC	0.8666	N.S	Yes	t-test
	C1%	0.1493	N.S	Yes	t-test
	C2%	0.1577	N.S	No	Mann-Whitney U
	C3%	0.2510	N.S	No	Mann-Whitney U
	C4%	0.2893	N.S	No	Mann-Whitney U

640 **Table A8: Results of statistical tests for habitat differences (between salt-flat: Sa, A. marina: Av and R. stylosa: Rh) for each measured parameter at each season. Parametric data were analysed using ANOVA, while Kruskal-Wallis tests were applied for non-parametric distributions. Then post-hoc tests were used to identify the differences (Mann-Whitney or Tukey). Significance levels are indicated as follows:  $p < 0.05$  (\*),  $p < 0.01$  (\*\*), and  $p < 0.001$  (\*\*\*); N.S = not significant.**

Season	Parameter	P_value	Significance	Parametric test	Test used	Post-hoc Result
WET	pH	0.0000	***	No	Mann-Whitney	Sa vs Av ; Sa vs Rh ; Av vs Rh
DRY	pH	0.0001	***	No	Mann-Whitney	Sa vs Av ; Sa vs Rh ; Av vs Rh
WET	Eh	0.0001	***	No	Mann-Whitney	Sa vs Av ; Sa vs Rh ; Av vs Rh
DRY	Eh	0.0000	***	Yes	Tukey	N/A
WET	Salinity	0.0000	***	No	Mann-Whitney	Sa vs Av ; Sa vs Rh ; Av vs Rh
DRY	Salinity	0.0000	***	No	Mann-Whitney	Sa vs Av ; Sa vs Rh ; Av vs Rh
WET	Temperature	0.0000	***	Yes	Tukey	N/A
DRY	Temperature	0.0013	**	No	Mann-Whitney	Sa vs Rh ; Av vs Rh
WET	a <sub>254</sub>	0.0005	***	Yes	Tukey	N/A
DRY	a <sub>254</sub>	0.0001	***	No	Mann-Whitney	Sa vs Av ; Sa vs Rh
WET	a <sub>350</sub>	0.0001	***	No	Mann-Whitney	Sa vs Av ; Sa vs Rh
DRY	a <sub>350</sub>	0.0001	***	No	Mann-Whitney	Sa vs Av ; Sa vs Rh
WET	a <sub>442</sub>	0.0002	***	No	Mann-Whitney	Sa vs Av ; Sa vs Rh
DRY	a <sub>442</sub>	0.0001	***	No	Mann-Whitney	Sa vs Av ; Sa vs Rh
WET	S <sub>275-295</sub>	0.0214	*	No	Mann-Whitney	Sa vs Rh
DRY	S <sub>275-295</sub>	0.0022	**	No	Mann-Whitney	Sa vs Av ; Sa vs Rh
WET	S <sub>350-400</sub>	0.0003	***	No	Mann-Whitney	Sa vs Av ; Sa vs Rh
DRY	S <sub>350-400</sub>	0.0002	***	No	Mann-Whitney	Sa vs Av ; Sa vs Rh
WET	SR	0.0015	**	No	Mann-Whitney	Sa vs Av ; Sa vs Rh
DRY	SR	0.0050	**	No	Mann-Whitney	Sa vs Av ; Sa vs Rh
WET	E <sub>2</sub> E <sub>3</sub>	0.0011	**	No	Mann-Whitney	Sa vs Av ; Sa vs Rh



DRY	E2E3	0.0002	***	No	Mann-Whitney	Sa vs Av ; Sa vs Rh
WET	E4E6	0.1327	N.S	Yes	Mann-Whitney	N/A
DRY	E4E6	0.2982	N.S	Yes	Mann-Whitney	N/A
WET	water_content	0.0000	***	No	Mann-Whitney	Sa vs Av ; Sa vs Rh ; Av vs Rh
DRY	water_content	0.0000	***	No	Mann-Whitney	Sa vs Av ; Sa vs Rh ; Av vs Rh
WET	Density	0.0000	***	No	Mann-Whitney	Sa vs Av ; Sa vs Rh ; Av vs Rh
DRY	Density	0.0000	***	Yes	Tukey	N/A
WET	FI	0.0123	*	No	Mann-Whitney	Sa vs Rh ; Av vs Rh
DRY	FI	0.0002	***	Yes	Tukey	N/A
WET	HIX	0.0000	***	No	Mann-Whitney	Sa vs Av ; Sa vs Rh ; Av vs Rh
DRY	HIX	0.0001	***	Yes	Tukey	N/A
WET	BIX	0.0001	***	No	Mann-Whitney	Sa vs Av ; Sa vs Rh ; Av vs Rh
DRY	BIX	0.0001	***	No	Mann-Whitney	Sa vs Av ; Sa vs Rh ; Av vs Rh
WET	COD	0.0088	**	No	Mann-Whitney	Sa vs Av
DRY	COD	0.0001	***	No	Mann-Whitney	Sa vs Av ; Sa vs Rh ; Av vs Rh
WET	Clay	0.4859	N.S	Yes	Mann-Whitney	N/A
DRY	Clay	0.0135	*	No	Mann-Whitney	Av vs Rh
WET	Silt	0.0254	*	Yes	Tukey	N/A
DRY	Silt	0.0005	***	No	Mann-Whitney	Sa vs Av ; Sa vs Rh ; Av vs Rh
WET	Sand	0.6358	N.S	No	Mann-Whitney	N/A
DRY	Sand	0.0058	**	No	Mann-Whitney	Sa vs Av ; Sa vs Rh
WET	SUVA	0.6366	N.S	Yes	Mann-Whitney	N/A
DRY	SUVA	0.0000	***	No	Mann-Whitney	Sa vs Av ; Sa vs Rh ; Av vs Rh
WET	TOC	0.0000	***	No	Mann-Whitney	Sa vs Av ; Sa vs Rh ; Av vs Rh
DRY	TOC	0.0000	***	No	Mann-Whitney	Sa vs Av ; Sa vs Rh ; Av vs Rh
WET	C1%	0.0000	***	Yes	Tukey	N/A
DRY	C1%	0.0008	***	Yes	Tukey	N/A
WET	C2%	0.0586	N.S	No	Mann-Whitney	N/A
DRY	C2%	0.0048	**	No	Mann-Whitney	Sa vs Av ; Sa vs Rh
WET	C3%	0.0027	**	Yes	Tukey	N/A
DRY	C3%	0.3052	N.S	No	Mann-Whitney	N/A
WET	C4%	0.2549	N.S	No	Mann-Whitney	N/A
DRY	C4%	0.1854	N.S	No	Mann-Whitney	N/A

#### Data availability

645 The dataset supporting this study has been deposited in Zenodo at <https://doi.org/10.5281/zenodo.17042320> (Mouras et al., 2025b).

#### Team list

Naïna Mouras<sup>1,2</sup>, Cyril Marchand<sup>1</sup>, Maximilien Mathian<sup>1</sup>, Hugues Lemonnier<sup>2,3</sup>



- 650 <sup>1</sup>Institute of Applied and Exact Sciences, University of New Caledonia, Noumea, New Caledonia  
<sup>2</sup>Ifremer, CNRS, IRD, Univ Nouvelle-Calédonie, Univ La Réunion, ENTROPIE, 98800 Nouméa, New Caledonia  
<sup>3</sup>MARBEC, Univ. Montpellier, CNRS, Ifremer, IRD, Sète, France

#### Authors contributions: CRediT

- NM:** Conceptualization, Methodology, Formal analysis, Investigation, Visualization, Writing- Original draft, Writing – review  
 655 and editing. **CM:** Conceptualization, Validation, Supervision, Writing – review and editing. **MM:** Formal analysis, Writing –  
 review and editing. **HL:** Conceptualization, Investigation, Supervision, Writing- Reviewing and Editing,

#### Competing interests

The authors declare that they have no conflict of interest.

#### Acknowledgements

- 660 The authors are grateful to Kapeliele Gututauava (University of New Caledonia) for technical assistance during the fieldwork.  
 We also thank Chloé Factou and Océane Tardivel for their help with laboratory analyses. Special thanks go to Sarah Louise  
 Robin for her valuable support during the writing process. The authors are thankful to Benjamin Oursel (Mediterranean  
 Institute of Oceanography) for his assistance and support with TOC analysis which was conducted in Toulon due to exceptional  
 circumstances affecting laboratory access in New Caledonia in May 2024. We also thank Cécile Dupouy and Stéphane  
 665 Mounier (Mediterranean Institute of Oceanography), for granting access to FDOM analysis equipment and the ProgMEEF  
 software. Finally, we thank the Laboratoire de Moyens Analytiques (LAMA) for providing access to their laboratories for  
 chemical analyses. The authors would like to thank Riccardo Rodolpho-Metalpa from IRD for his invaluable help in providing  
 access to the field, and Thierry for his welcoming in his property.

#### Financial support

- 670 This work was part of Mouras Naïna's PhD funded by the University of New Caledonia. This study was supported by  
 TROPICOS of the exploratory research program FairCarboN (ANR-22-PEXF-00012). This work was also undertaken within  
 the PRESENCE (PRESSures on coral Ecosystems of New CalEdonia) scientific project, sponsored by the New Caledonia  
 institutions (Government, South Province, North Province).

#### References

- 675 Adame, M., Reef, R., Santini, N., Najera, E., Turschwell, M., Hayes, M., Masque, P., & Lovelock, C. (2021). Mangroves in arid  
 regions: Ecology, threats, and opportunities. *Estuarine Coastal And Shelf Science*, 248, 106796.  
<https://doi.org/10.1016/j.ecss.2020.106796>  
 Adame, M. F., Cormier, N., Taillardat, P., Iram, N., Rovai, A., Sloey, T. M., Yando, E. S., Blanco-Libreros, J. F., Arnaud, M.,  
 Jennerjahn, T., Lovelock, C. E., Friess, D., Reithmaier, G. M. S., Buelow, C. A., Muhammad-Nor, S. M., Twilley, R.  
 680 R., & Ribeiro, R. A. (2024). Deconstructing the mangrove carbon cycle: Gains, transformation, and losses. *Ecosphere*,  
 15(3). <https://doi.org/10.1002/ecs2.4806>



- Alessi, C., Lemonnier, H., Camp, E. F., Wabete, N., Payri, C., & Metalpa, R. R. (2024). Algal symbiont diversity in *Acropora muricata* from the extreme reef of Bouraké associated with resistance to coral bleaching. *PLoS ONE*, 19(2), e0296902. <https://doi.org/10.1371/journal.pone.0296902>
- 685 Alongi, D. M., de Carvalho, N. A., Amaral, A. L., da Costa, A., Trott, L., & Tirendi, F. (2012). Uncoupled surface and below-ground soil respiration in mangroves: Implications for estimates of dissolved inorganic carbon export. *Biogeochemistry*, 109(1–3), 151–162. <https://doi.org/10.1007/s10533-011-9616-9>
- Alongi, D. M. (2014). Carbon cycling and storage in mangrove forests. *Annual Review of Marine Science*, 6, 195–219. <https://doi.org/10.1146/annurev-marine-010213-135020>
- 690 Alongi, D. M. (2022). Lateral Export and Sources of Subsurface Dissolved Carbon and Alkalinity in Mangroves: Revising the Blue Carbon Budget. *Journal Of Marine Science And Engineering*, 10(12), 1916. <https://doi.org/10.3390/jmse10121916>
- Amaral, V., Romera-Castillo, C., & Forja, J. (2020). Dissolved Organic Matter in the Gulf of Cádiz: Distribution and Drivers of Chromophoric and Fluorescent Properties. *Frontiers in Marine Science*, 7. <https://doi.org/10.3389/fmars.2020.00126>
- 695 Amon, R. M. W., & Benner, R. (1994). Rapid cycling of high-molecular-weight dissolved organic matter in the ocean. *Nature*, 369(6481), 549–552. <https://doi.org/10.1038/369549a0>
- Arnaud, M., Krause, S., Norby, R. J., Dang, T. H., Acil, N., Kettridge, N., Gauci, V., & Ullah, S. (2023). Global mangrove root production, its controls and roles in the blue carbon budget of mangroves. *Global Change Biology*, 29(12), 3256–3270. <https://doi.org/10.1111/gcb.16701>
- 700 Arrigo, K., & Brown, C. (1996). Impact of chromophoric dissolved organic matter on UV inhibition of primary productivity in the sea. *Marine Ecology Progress Series*, 140, 207–216. <https://doi.org/10.3354/meps140207>
- Ball, M. C. (1998). Mangrove Species Richness in Relation to Salinity and Waterlogging: A Case Study Along the Adelaide River Floodplain, Northern Australia (Vol. 7, Issue 1).
- Baltzer, F. (1982). Géodynamique de la sédimentation et diagenèse précoce en domaine ultrabasique Nouvelle-Calédonie (Travaux et Documents de l'ORSTOM, No. 152, p. 283). ORSTOM.
- 705 Bro, R. (1997). PARAFAC. Tutorial and applications. *Chemometrics and Intelligent Laboratory Systems*, 38(2), 149–171. [https://doi.org/10.1016/S0169-7439\(97\)00032-4](https://doi.org/10.1016/S0169-7439(97)00032-4)
- Barhoumi, Z., Hussain, A. A., & Atia, A. (2021). Physiological response of *Avicennia marina* to salinity and recovery. *Russian Journal of Plant Physiology*, 68(4), 696–707. <https://doi.org/10.1134/S102144372104004X>
- 710 Butturini, A., Herzsprung, P., Lechtenfeld, O., Alcorlo, P., Benaiges-Fernandez, R., Berlanga, M., Boadella, J., Campillo, Z. F., Gomez, R., Sanchez-Montoya, M., Urmeneta, J., & Romaní, A. (2022). Origin, accumulation and fate of dissolved organic matter in an extreme hypersaline shallow lake. *Water Research*, 221, 118727. <https://doi.org/10.1016/j.watres.2022.118727>
- Cabral, A., Reithmaier, G. M. S., Yau, Y. Y. Y., Cotovicz, L. C., Barreira, J., Viana, B., Hayden, J., Bouillon, S., Brandini, N., Hatje, V., De Rezende, C. E., Fonseca, A. L., & Santos, I. R. (2024). Large Porewater-Derived Carbon Outwelling Across Mangrove Seascapes Revealed by Radium Isotopes. *Journal Of Geophysical Research Oceans*, 129(9). <https://doi.org/10.1029/2024jc021319>
- 715 Cawley, K. M., Yamashita, Y., Maie, N., & Jaffé, R. (2014). Using Optical Properties to Quantify Fringe Mangrove Inputs to the Dissolved Organic Matter (DOM) Pool in a Subtropical Estuary. *Estuaries and Coasts*, 37(2), 399–410. <https://doi.org/10.1007/s12237-013-9681-5>
- 720 Chen, M., Kim, S. H., Jung, H. J., Hyun, J. H., Choi, J. H., Lee, H. J., Huh, I. A., & Hur, J. (2017). Dynamics of dissolved organic matter in riverine sediments affected by weir impoundments: Production, benthic flux, and environmental implications. *Water Research*, 121, 150–161. <https://doi.org/10.1016/j.watres.2017.05.022>



- Chow, A. T. S., Ulus, Y., Huang, G., Kline, M. A., & Cheah, W. Y. (2022). Challenges in quantifying and characterizing dissolved organic carbon: Sampling, isolation, storage, and analysis. In *Journal of Environmental Quality* (Vol. 51, Issue 5, pp. 837–871). John Wiley and Sons Inc. <https://doi.org/10.1002/jeq2.20392>
- Chowdhury, R., Sutradhar, T., Begam, M. M., Mukherjee, C., Chatterjee, K., Basak, S. K., & Ray, K. (2019). Effects of nutrient limitation, salinity increase, and associated stressors on mangrove forest cover, structure, and zonation across Indian Sundarbans. *Hydrobiologia*, 842(1), 191–217. <https://doi.org/10.1007/s10750-019-04036-9>
- Clark, M. W., McConchie, D., Lewis, D. W., & Saenger, P. (1998). Redox stratification and heavy metal partitioning in *Avicennia*-dominated mangrove sediments: A geochemical model. *Chemical Geology*, 149, 147–171. [https://doi.org/10.1016/S0009-2541\(98\)00034-5](https://doi.org/10.1016/S0009-2541(98)00034-5)
- Coble, P. G. (1996). Characterization of marine and terrestrial DOM in seawater using excitation-emission matrix spectroscopy. In *Marine Chemistry* (Vol. 51).
- Coble, P. G. (2007). Marine optical biogeochemistry: The chemistry of ocean color. *Chemical Reviews*, 107(2), 402–418. <https://doi.org/10.1021/cr050350+>
- Deborde, J., Marchand, C., Molnar, N., Patrona, L. Della, & Meziane, T. (2015). Concentrations and fractionation of carbon, iron, sulfur, nitrogen and phosphorus in mangrove sediments along an intertidal gradient (Semi-Arid Climate, New Caledonia). *Journal of Marine Science and Engineering*, 3(1), 52–72. <https://doi.org/10.3390/jmse3010052>
- Dittmar, T., Hertkorn, N., Kattner, G., & Lara, R. J. (2006). Mangroves, a major source of dissolved organic carbon to the oceans. *Global Biogeochemical Cycles*, 20(1), 1–7. <https://doi.org/10.1029/2005GB002570>
- Dittmar, T., & Lara, R. J. (2001). Driving forces behind nutrient and organic matter dynamics in a mangrove tidal creek in North Brazil. *Estuarine, Coastal and Shelf Science*, 52(2), 249–259. <https://doi.org/10.1006/ecss.2000.0743>
- Donato, D. C., Kauffman, J. B., Murdiyarso, D., Kurnianto, S., Stidham, M., & Kanninen, M. (2011). Mangroves among the most carbon-rich forests in the tropics. *Nature Geoscience*, 4(5), 293–297. <https://doi.org/10.1038/ngeo1123>
- Douillet, P. (2001). Atlas hydrodynamique du lagon sud-ouest de Nouvelle-Calédonie.
- Dubuc, A., Baker, R., Marchand, C., Waltham, N. J., & Sheaves, M. (2019). Hypoxia in mangroves: Occurrence and impact on valuable tropical fish habitat. *Biogeosciences*, 16(20), 3959–3976. <https://doi.org/10.5194/bg-16-3959-2019>
- Duke, N. C., Ball, M. C., & Ellison, J. C. (1998). Factors influencing biodiversity and distributional gradients in mangroves. *Global Ecology and Biogeography Letters*, 7(1), 27–47. <https://doi.org/10.2307/2997695>
- Garcia, J. D. S., Dalmolin, Â. C., França, M. G. C., & Mangabeira, P. A. O. (2017). Different salt concentrations induce alterations both in photosynthetic parameters and salt gland activity in leaves of the mangrove *Avicennia schaueriana*. *Ecotoxicology And Environmental Safety*, 141, 70–74. <https://doi.org/10.1016/j.ecoenv.2017.03.016>
- Gee, G.W. and Bauder, J.W. (1986) Particle-Size Analysis. In: Klute, A., Ed., *Methods of Soil Analysis, Part 1. Physical and Mineralogical Methods*, Agronomy Monograph No. 9, 2nd Edition, American Society of Agronomy/Soil Science Society of America, Madison, WI, 383–411.
- Ghabban, H., Albalawi, D. A., Al-Otaibi, A. S., Alshehri, D., Alenzi, A. M., Alatawy, M., Alatawi, H. A., Alnagar, D. K., & Bahieldin, A. (2024). Investigating the bacterial community of gray mangroves (*Avicennia marina*) in coastal areas of Tabuk region. *PeerJ*, 12(10). <https://doi.org/10.7717/peerj.18282>
- Giri, C., Ochieng, E., Tieszen, L. L., Zhu, Z., Singh, A., Loveland, T., Masek, J., & Duke, N. (2011). Status and distribution of mangrove forests of the world using earth observation satellite data. *Global Ecology and Biogeography*, 20(1), 154–159. <https://doi.org/10.1111/j.1466-8238.2010.00584.x>
- Gonsior, M., Schmitt-Kopplin, P., & Bastviken, D. (2013). Depth-dependent molecular composition and photo-reactivity of dissolved organic matter in a boreal lake under winter and summer conditions. *Biogeosciences*, 10(11), 6945–6956. <https://doi.org/10.5194/bg-10-6945-2013>



- Groeneveld, M., Catalán, N., Attermeyer, K., Hawkes, J., Einarsdóttir, K., Kothawala, D., Bergquist, J., & Tranvik, L. (2020). Selective Adsorption of Terrestrial Dissolved Organic Matter to Inorganic Surfaces Along a Boreal Inland Water Continuum. *Journal Of Geophysical Research Biogeosciences*, 125(3). <https://doi.org/10.1029/2019jg005236>
- 770 Hansen, A. M., Kraus, T. E. C., Pellerin, B. A., Fleck, J. A., Downing, B. D., & Bergamaschi, B. A. (2016). Optical properties of dissolved organic matter (DOM): Effects of biological and photolytic degradation. *Limnology and Oceanography*, 61(3), 1015–1032. <https://doi.org/10.1002/lno.10270>
- Haro, S., Mucheye, T., Caballero, I., Priego, B., Gonzalez, C. J., Gómez-Ramírez, E. H., Corzo, A., & Papaspyrou, S. (2025). Microphytobenthos spatio-temporal dynamics across an intertidal gradient in a tropical estuary using Sentinel-2 imagery. *Science of The Total Environment*, 963, 178516. <https://doi.org/10.1016/j.scitotenv.2025.178516>
- 775 Hautala, K., Peuravuori, J., & Pihlaja, K. (2000). Measurement of aquatic humus content by spectroscopic analyses. *Water Research*, 34(1), 246–258. [https://doi.org/10.1016/S0043-1354\(99\)00137-2](https://doi.org/10.1016/S0043-1354(99)00137-2)
- Helms, J., Stubbins, A., Ritchie, J. D., Minor, E. C., Kieber, D. J., & Mopper, K. (2008). Absorption spectral slopes and slope ratios as indicators of molecular weight, source, and photobleaching of chromophoric dissolved organic matter (*Limnology and Oceanography* 53 955-969). *Limnology and Oceanography*, 54(3), 1023. <https://doi.org/10.4319/lno.2009.54.3.1023>
- 780 Hinsinger, P., Plassard, C., Tang, C., & Jaillard, B. (2003). Origins of root-mediated pH changes in the rhizosphere and their responses to environmental constraints: A review. *Plant and Soil*, 248, 43-59. <https://doi.org/10.1023/A:1022371130939>
- Hoff, M., Brisse, H., & Grandjouan, G. (1983). La végétation rudérale et anthropique de la Nouvelle-Calédonie et des îles Loyauté (Pacifique sud).
- 785 Hong, H., Wu, S., Wang, Q., Dai, M., Qian, L., Zhu, H., Li, J., Zhang, J., Liu, J., Li, J., Lu, H., & Yan, C. (2021). Fluorescent dissolved organic matter facilitates the phytoavailability of copper in the coastal wetlands influenced by artificial topography. *Science of the Total Environment*, 790. <https://doi.org/10.1016/j.scitotenv.2021.147855>
- Huguet, A., Vacher, L., Relexans, S., Saubusse, S., Froidefond, J. M., & Parlanti, E. (2009). Properties of fluorescent dissolved organic matter in the Gironde Estuary. *Organic Geochemistry*, 40(6), 706–719. <https://doi.org/10.1016/j.orggeochem.2009.03.002>
- 790 Jacotot, A., Marchand, C., & Allenbach, M. (2018). Biofilm and temperature controls on greenhouse gas (CO<sub>2</sub> and CH<sub>4</sub>) emissions from a *Rhizophora* mangrove soil (New Caledonia). *The Science Of The Total Environment*, 650, 1019-1028. <https://doi.org/10.1016/j.scitotenv.2018.09.093>
- 795 Kathiresan, K., Anburaj, R., Gomathi, V., & Saravanakumar, K. (2013). Carbon sequestration potential of *Rhizophora mucronata* and *Avicennia marina* as influenced by age, season, growth and sediment characteristics in southeast coast of India. *Journal of Coastal Conservation*, 17(3), 397–408. <https://doi.org/10.1007/s11852-013-0236-5>
- Kida, M., Watanabe, I., Kinjo, K., Kondo, M., Yoshitake, S., Tomotsune, M., Iimura, Y., Umnouysin, S., Suchewaboripont, V., Pongpam, S., Ohtsuka, T., & Fujitake, N. (2021). Organic carbon stock and composition in 3.5-m core mangrove soils (Trat, Thailand). *Science of the Total Environment*, 801. <https://doi.org/10.1016/j.scitotenv.2021.149682>
- 800 Kristensen, E., Bouillon, S., Dittmar, T., & Marchand, C. (2008). Organic carbon dynamics in mangrove ecosystems: A review. In *Aquatic Botany* (Vol. 89, Issue 2, pp. 201–219). <https://doi.org/10.1016/j.aquabot.2007.12.005>
- Kristensen, E., Connolly, R.M., Otero, X.L., Marchand, C., Ferreira, T.O., Rivera-Monroy, V.H. (2017). Biogeochemical Cycles: Global Approaches and Perspectives. In: Rivera-Monroy, V., Lee, S., Kristensen, E., Twilley, R. (eds) *Mangrove Ecosystems: A Global Biogeographic Perspective*. Springer, Cham. [https://doi.org/10.1007/978-3-319-62206-4\\_6](https://doi.org/10.1007/978-3-319-62206-4_6)
- 805





- Lambert, T., Bouillon, S., Darchambeau, F., Massicotte, P., & Borges, A. V. (2016). Shift in the chemical composition of dissolved organic matter in the Congo River network. *Biogeosciences*, 13(18), 5405–5420. <https://doi.org/10.5194/bg-13-5405-2016>
- 810 Leopold, A., Marchand, C., Deborde, J., Chaduteau, C., & Allenbach, M. (2013). Influence of mangrove zonation on CO<sub>2</sub> fluxes at the sediment–air interface (New Caledonia). *Geoderma*, 202–203, 62–70. <https://doi.org/10.1016/j.geoderma.2013.03.008>
- Leopold, A., Marchand, C., Deborde, J., & Allenbach, M. (2015). Temporal variability of CO<sub>2</sub> fluxes at the sediment–air interface in mangroves (New Caledonia). *The Science Of The Total Environment*, 502, 617–626. <https://doi.org/10.1016/j.scitotenv.2014.09.066>
- 815 Leopold, A., Marchand, C., Renchon, A., Deborde, J., Quiniou, T., & Allenbach, M. (2016). Net ecosystem CO<sub>2</sub> exchange in the “Coeur de Voh” mangrove, New Caledonia: Effects of water stress on mangrove productivity in a semi-arid climate. *Agricultural and Forest Meteorology*, 223, 217–232. <https://doi.org/10.1016/j.agrformet.2016.04.006>
- Leopold, A., Marchand, C., Deborde, J. et al. Water Biogeochemistry of a Mangrove-Dominated Estuary Under a Semi-Arid Climate (New Caledonia). *Estuaries and Coasts* 40, 773–791 (2017). <https://doi.org/10.1007/s12237-016-0179-9>
- 820 Loo, Y. P., Ouyang, X., Lai, D. Y. F., & Lee, S. Y. (2024). The Microphytobenthos are Abundant and Mediate Key Carbon Fluxes in Tropical Mangroves. *Estuaries And Coasts*, 47(4), 963–980. <https://doi.org/10.1007/s12237-024-01339-6>
- Lv, J., Zhang, S., Wang, S., Luo, L., Cao, D., & Christie, P. (2016). Molecular-Scale Investigation with ESI-FT-ICR-MS on Fractionation of Dissolved Organic Matter Induced by Adsorption on Iron Oxyhydroxides. *Environmental Science & Technology*, 50(5), 2328–2336. <https://doi.org/10.1021/acs.est.5b04996>
- 825 Maie, N., Pisani, O., & Jaffé, R. (2008). Mangrove tannins in aquatic ecosystems: Their fate and possible influence on dissolved organic carbon and nitrogen cycling. *Limnology and Oceanography*, 53(1), 160–171. <https://doi.org/10.4319/lo.2008.53.1.0160>
- Maie, N., Yamashita, Y., Cory, R. M., Boyer, J. N., & Jaffé, R. (2012). Application of excitation emission matrix fluorescence monitoring in the assessment of spatial and seasonal drivers of dissolved organic matter composition: Sources and physical disturbance controls. *Applied Geochemistry*, 27(4), 917–929. <https://doi.org/10.1016/j.apgeochem.2011.12.021>
- 830 Marchand, C., Albéric, P., Lallier-Vergès, E., & Baltzer, F. (2006). Distribution and characteristics of dissolved organic matter in mangrove sediment pore waters along the coastline of French Guiana. *Biogeochemistry*, 81(1), 59–75. <https://doi.org/10.1007/s10533-006-9030-x>
- 835 Marchand, C., Allenbach, M., & Lallier-Vergès, E. (2011). Relationships between heavy metals distribution and organic matter cycling in mangrove sediments (Conception Bay, New Caledonia). *Geoderma*, 160(3–4), 444–456. <https://doi.org/10.1016/j.geoderma.2010.10.015>
- Marchand, C., Fernandez, J. M., & Moreton, B. (2016). Trace metal geochemistry in mangrove sediments and their transfer to mangrove plants (New Caledonia). *Science of the Total Environment*, 562, 216–227. <https://doi.org/10.1016/j.scitotenv.2016.03.206>
- 840 Marchand, C., Fernandez, J. M., Moreton, B., Landi, L., Lallier-Vergès, E., & Baltzer, F. (2012). The partitioning of transitional metals (Fe, Mn, Ni, Cr) in mangrove sediments downstream of a ferrallitized ultramafic watershed (New Caledonia). *Chemical Geology*, 300–301, 70–80. <https://doi.org/10.1016/j.chemgeo.2012.01.018>
- 845 McKnight, D. M., Boyer, E. W., Westerhoff, P. K., Doran, P. T., Kulbe, T., & Andersen, D. T. (2001). Spectrofluorometric characterization of dissolved organic matter for indication of precursor organic material and aromaticity. *Limnology and Oceanography*, 46(1), 38–48. <https://doi.org/10.4319/lo.2001.46.1.0038>



- Meyneng, M., Siano, R., Mouras, N., Ansquer, D., Laporte-Magoni, C., Antypas, F., Haize, T., & Lemonnier, H. (2024). The Origin of the Matter Matters: The Influence of Terrestrial Inputs on Coastal Benthic Microeukaryote Communities Revealed by eDNA. *Environmental DNA*, 6(6), e70041. <https://doi.org/10.1002/edn3.7004>
- 850 Molnar, N., Marchand, C., Deborde, J., Della Patrona, L., & Meziane, T. (2014). Seasonal Pattern of the Biogeochemical Properties of Mangrove Sediments Receiving Shrimp Farm Effluents (New Caledonia). *Journal Of Aquaculture Research & Development*, 05(05). <https://doi.org/10.4172/2155-9546.1000262>
- Mounier, S., Zhao, H., Garnier, C., & Redon, R. (2011). Copper complexing properties of dissolved organic matter : PARAFAC treatment of fluorescence quenching. *Biogeochemistry*, 106(1), 107-116. <https://doi.org/10.1007/s10533-010-9486-6>
- 855 Mouras, N., Lemonnier, H., Crossay, T., Gututauava, K., Mathian, M., Robin, S. L., Tardivel, O., & Marchand, C. (2025a). Variability of the optical signatures of dissolved organic matter in soils of different mangrove stands (Ouvéa, New Caledonia). *Environmental Science and Pollution Research*. <https://doi.org/10.1007/s11356-025-36373-9>
- Mouras, N., Marchand, C., Mathian, M., & Lemonnier, H. (2025b). Seasonal dynamics of dissolved organic matter along an intertidal gradient in semi-arid mangrove soils (New Caledonia) [Data set]. Zenodo. <https://doi.org/10.5281/zenodo.17042320>
- 860 Noël, V., Marchand, C., Juillot, F., Ona-Nguema, G., Viollier, E., Marakovic, G., Olivi, L., Delbes, L., Gelebart, F., & Morin, G. (2014). EXAFS analysis of iron cycling in mangrove sediments downstream a lateritized ultramafic watershed (Vavouto Bay, New Caledonia). *Geochimica et Cosmochimica Acta*, 136, 211-228. <https://doi.org/10.1016/j.gca.2014.03.019>
- 865 Ohtsuka, T., Onishi, T., Yoshitake, S., Tomotsune, M., Kida, M., Iimura, Y., Kondo, M., Suchewaboripont, V., Cao, R., Kinjo, K., & Fujitake, N. (2020). Lateral export of dissolved inorganic and organic carbon from a small mangrove estuary with tidal fluctuation. *Forests*, 11(10), 1–15. <https://doi.org/10.3390/f11101041>
- Parlanti, E., Wörz, K., Geoffroy, L., & Lamotte, M. (2000). Dissolved organic matter fluorescence spectroscopy as a tool to estimate biological activity in a coastal zone submitted to anthropogenic inputs. *Organic Geochemistry*, 31(12), 1765–1781. [https://doi.org/10.1016/S0146-6380\(00\)00124-8](https://doi.org/10.1016/S0146-6380(00)00124-8)
- 870 Ray, R., Miyajima, T., Watanabe, A., Yoshikai, M., Ferrera, C. M., Orizar, I., Nakamura, T., Diego-McGlone, M. L. S., Herrera, E. C., & Nadaoka, K. (2021). Dissolved and particulate carbon export from a tropical mangrove-dominated riverine system. *Limnology And Oceanography*, 66(11), 3944-3962. <https://doi.org/10.1002/lno.11934>
- 875 Robin, S. L., Baudin, F., Le Milbeau, C., & Marchand, C. (2024a). Millennial-aged organic matter preservation in anoxic and sulfidic mangrove soils: Insights from isotopic and molecular analyses. *Estuarine, Coastal and Shelf Science*, 308. <https://doi.org/10.1016/j.ecss.2024.108936>
- Robin, S. L., Le Milbeau, C., Gututauava, K., & Marchand, C. (2024b). Influence of species and stand position on isotopic and molecular composition of leaf litter during degradation in an urban mangrove forest. *Geochimica et Cosmochimica Acta*, 372, 1-12. <https://doi.org/10.1016/j.gca.2024.03.008>
- 880 Rocha, J. C., Sargentini, É., Toscano, I. A. S., Rosa, A. H., & Burba, P. (1999). Multi-method Study on Aquatic Humic Substances from the “Rio Negro” - Amazonas State/Brazil. Emphasis on Molecular-Size Classification of their Metal Contents. *Journal of the Brazilian Chemical Society*, 10(3), 169–175. <https://doi.org/10.1590/S0103-50531999000300002>
- 885 Santín, C., Yamashita, Y., Otero, X. L., Álvarez, M. Á., & Jaffé, R. (2009). Characterizing humic substances from estuarine soils and sediments by excitation-emission matrix spectroscopy and parallel factor analysis. *Biogeochemistry*, 96(1), 131–147. <https://doi.org/10.1007/s10533-009-9349-1>
- Sanyal, P., Ray, R., Paul, M., Gupta, V. K., Acharya, A., Bakshi, S., Jana, T. K., & Mukhopadhyay, S. K. (2020). Assessing the Dynamics of Dissolved Organic Matter (DOM) in the Coastal Environments Dominated by Mangroves, Indian Sundarbans. *Frontiers in Earth Science*, 8. <https://doi.org/10.3389/feart.2020.00218>
- 890



- Shank, G. C., Lee, R., Vähätalo, A., Zepp, R. G., & Bartels, E. (2010). Production of chromophoric dissolved organic matter from mangrove leaf litter and floating Sargassum colonies. *Marine Chemistry*, 119(1–4), 172–181. <https://doi.org/10.1016/j.marchem.2010.02.002>
- Ullmann, C. V., Campbell, H. J., Frei, R., & Korte, C. (2014). Geochemical signatures in Late Triassic brachiopods from New Caledonia. *New Zealand Journal of Geology and Geophysics*, 57(4), 420–431. <https://doi.org/10.1080/00288306.2014.958175>
- Vinh, T., Allenbach, M., Joanne, A., & Marchand, C. (2019). Seasonal variability of CO<sub>2</sub> fluxes at different interfaces and vertical CO<sub>2</sub> concentration profiles within a Rhizophora mangrove forest (Can Gio, Viet Nam). *Atmospheric Environment*, 201, 301–309. <https://doi.org/10.1016/j.atmosenv.2018.12.049>
- 900 Wang, H., Ke, H., Wu, H., Ma, S., Altaf, M. M., & Diao, X. (2024). Season shapes the functional diversity of microbial carbon metabolism in mangrove soils of Hainan Island, China. *CATENA*, 235, 107710. <https://doi.org/10.1016/j.catena.2023.107710>
- Wauthy, M., Rautio, M., Christoffersen, K. S., Forsström, L., Laurion, I., Mariash, H. L., Peura, S., & Vincent, W. F. (2018). Increasing dominance of terrigenous organic matter in circumpolar freshwaters due to permafrost thaw. *Limnology And Oceanography Letters*, 3(3), 186–198. <https://doi.org/10.1002/lol2.10063>
- 905 Xiao, K., Zhang, P., Santos, I. R., Wang, J., Li, Z., Wang, X., Wang, Y., Lu, M., Zhang, L., & Li, H. (2023). Tidal Pumping Controls Dissolved Organic Matter Properties and Outwelling From Mangrove Groundwater to Coastal Water. *Water Resources Research*, 59(3). <https://doi.org/10.1029/2022wr033913>
- Yamashita, Y., & Jaffé, R. (2008). Characterizing the interactions between trace metals and dissolved organic matter using excitation-emission matrix and parallel factor analysis. *Environmental Science and Technology*, 42(19), 7374–7379. <https://doi.org/10.1021/es801357h>
- 910 Yamashita, Y., & Tanoue, E. (2009). Basin scale distribution of chromophoric dissolved organic matter in the Pacific Ocean. *Limnology and Oceanography*, 54(2), 598–609. <https://doi.org/10.4319/lo.2009.54.2.0598>
- Yin, S., Wang, J., Yu, T., Wang, M., Wu, Y., & Zeng, H. (2023). Constraints on the spatial variations of soil carbon fractions in a mangrove forest in Southeast China. *CATENA*, 222, 106889. <https://doi.org/10.1016/j.catena.2022.106889>
- 915 Zepp, R. G., Sheldon, W. M., & Moran, M. A. (2004). Dissolved organic fluorophores in southeastern US coastal waters: Correction method for eliminating Rayleigh and Raman scattering peaks in excitation-emission matrices. *Marine Chemistry*, 89(1–4), 15–36. <https://doi.org/10.1016/j.marchem.2004.02.006>
- Zhu, W. Z., Wang, S. H., Wang, D. Z., Feng, W. H., Li, B., & Zhang, H. H. (2023). Contrasting effects of different light regimes on the photoreactivities of allochthonous and autochthonous chromophoric dissolved organic matter. *Chemosphere*, 332. <https://doi.org/10.1016/j.chemosphere.2023.138823>
- 920